

NPS ARCHIVE
1966
FIGUEIREDO, A.

**A PHOTO-ELASTIC STUDY OF STRESS DISTRIBUTION
IN SHIP TRANSVERSE BULKHEADS**

Arthur Ramos Figueiredo
Daniel Angelo Marangiello
and
Walter Vilela Guerra

DUDLEY KNOX LIBRARY
NAVAL POSTGRADUATE SCHOOL
MONTEREY CA 93943-5101

Library
U. S. Naval Postgraduate School
Monterey, California

2547

209A 29N
1961
A, 0601507

**A PHOTO-ELASTIC STUDY OF STRESS DISTRIBUTION
IN SHIP TRANSVERSE BULKHEADS**

by

ARTHUR RAMOS FIGUEIREDO

and

DANIEL ANGELO MARANGIELLO

**SUBMITTED IN PARTIAL FULFILLMENT OF THE
REQUIREMENTS FOR THE DEGREE OF
NAVAL ENGINEER**

and

WALTER VILELA GUERRA

**SUBMITTED IN PARTIAL FULFILLMENT OF THE
REQUIREMENTS FOR THE DEGREE OF
MASTER OF SCIENCE IN
NAVAL ARCHITECTURE AND
MARINE ENGINEERING**

at the

**MASSACHUSETTS INSTITUTE OF TECHNOLOGY
MAY 1956**

1966
Figueiredo, A.

F425

RECEIVED THE BUREAU OF THE SECRETARY OF THE ARMY
WASHINGTON, D. C. 20315

TO
THE SECRETARY OF THE ARMY

FROM

THE SECRETARY OF THE ARMY

RE: THE SECRETARY OF THE ARMY
TO THE SECRETARY OF THE ARMY
WASHINGTON, D. C. 20315

DATE

THE SECRETARY OF THE ARMY

RE: THE SECRETARY OF THE ARMY
TO THE SECRETARY OF THE ARMY
WASHINGTON, D. C. 20315

END

WASHINGTON, D. C. 20315
JAN 1966

A PHOTO-ELASTIC STUDY OF THE STRESS DISTRIBUTION
IN SHIP TRANSVERSE BULKHEADS

by

ARTHUR RAMOS FIGUEIREDO

and

DANIEL ANGELO MARANGIELLO

Submitted to the Department of Naval Architecture
and Marine Engineering on 21 May 1956 in partial
fulfillment of the requirements for the degree of
Naval Engineer

and

WALTER VILELA GUERRA

Submitted to the Department of Naval Architecture
and Marine Engineering on 21 May 1956 in partial
fulfillment of the requirements for the degree of
Master of Science in Naval Architecture and Marine
Engineering

ABSTRACT

This thesis is a continuation of the work of Rockwell Holman, reference (13). The general objective is the determination of data pertinent to the design of ship transverse bulkheads. Specifically, this thesis investigates the distribution of load between side and bottom supports for an unstiffened bulkhead subjected to a concentrated load applied centrally in its plane. The effect of a vertical centerline stiffener on this distribution is also investigated.

The photo-elastic approach was used and the Shear Difference method employed in computing the shear stress distribution over the side support.

Two rectangular plates of identical dimensions were used. Isochromatics were recorded by photographing the loaded Catalin 61-893 plate. Isoclinics were obtained by tracing the pattern shown on the less sensitive Plexiglass plate.

Curves were obtained for the shear stress distribution at the sides for the unstiffened plate supported at sides only, and at sides and bottom; and for the stiffened plate supported at sides and bottom.

Overall accuracy was determined to be within 10%.

A FURTHER STUDY OF THE ALGAL FLORA OF

THE ALGAL FLORA OF

BY

ALFRED HENRY HENNING

AND

ALFRED HENRY HENNING

Submitted to the Department of Botany
and Marine Biology in partial fulfillment
of the requirements for the degree of
Doctor of Philosophy

1915

ALFRED HENRY HENNING

Submitted to the Department of Botany
and Marine Biology in partial fulfillment
of the requirements for the degree of
Doctor of Philosophy in Botany and Marine
Biology

ALFRED

This thesis is a contribution to the work of the Botanical Museum

The addition of the stiffener had little effect on the shape of the shear distribution, but it reduced appreciably the part of the load taken by the bottom.

The validity of these results should be investigated further by photo-elastic studies using plates of various aspect ratios with several stiffener arrangements.

Thesis Supervisor: William M. Murray

Title: Professor of Mechanical Engineering

The addition of the element has little effect on the shape of the glass distribution, but it reduces appreciably the part of the curve taken by the bottom.

The validity of these results should be investigated further by hydrostatic studies using glasses of various types tested with several different arrangements.

It is to be noted that the results obtained in the present study are in good agreement with those obtained in the study of the effect of the addition of the element on the shape of the glass distribution.

The results obtained in the present study are in good agreement with those obtained in the study of the effect of the addition of the element on the shape of the glass distribution.

The results obtained in the present study are in good agreement with those obtained in the study of the effect of the addition of the element on the shape of the glass distribution.

These results are in good agreement with those obtained in the study of the effect of the addition of the element on the shape of the glass distribution.

The results obtained in the present study are in good agreement with those obtained in the study of the effect of the addition of the element on the shape of the glass distribution.

ACKNOWLEDGMENT

The authors wish to express their appreciation to Professor William M. Murray of the Department of Mechanical Engineering for permission to use the facilities of the Experimental Stress Analysis Laboratory and for his invaluable assistance, to Professor J. Harvey Evans, for suggesting the investigation and allowing the use of test equipment from the Ships Structure Laboratory, and to Mr. Jerome Catz for his advice on instrumentation and laboratory procedure.

MEMORANDUM

The subject is to express their appreciation to Professor
William H. Murray of the Department of Medical Engineering for
permission to use the facilities of the Department of
Anatomy Laboratory and for his invaluable assistance, as Professor
J. Murray Brown, for suggesting the investigation and allowing the
use of part of his time from the High Research Laboratory, and to
Mr. Thomas Lee for his advice on instrumentation and laboratory
procedures.

Cambridge, Massachusetts
May 21, 1956

Secretary of the Faculty
Massachusetts Institute of Technology
Cambridge 39, Massachusetts

Dear Sir:

In accordance with the requirements for the Degrees of Naval Engineer and Master of Science in Naval Architecture and Marine Engineering, we herewith submit a thesis entitled: "A Photo-Elastic Study of Stress Distribution in Ship Transverse Bulkheads".

Respectfully yours,

1951, 1952

in accordance with the requirements for the Degree of Master
of Science in Naval Architecture and Marine Engineering,
as prescribed by the Board of Engineers, United States Navy,
and as approved by the Department of the Navy.

Very truly yours,
[Signature]

Chief of Bureau

TABLE OF CONTENTS

	<u>Page</u>
I Introduction	1
II Procedure.....	5
III Results	7
IV Discussion of Results	9
V Conclusions	13
VI Recommendations	14
VII Appendix	15
A. Supplementary Introduction	16
B. Details of Procedure	24
C. Original Data and Calculations	40
D. Literature Citations	67

TABLE OF CONTENTS

Page

I	Introduction	I
II	Procedures	II
III	Results	III
IV	Discussion and Conclusions	IV

I. INTRODUCTION

Whenever a structure is being designed all efforts are made by the designer toward a least weight solution that still fulfills the safety requirements. A solution of this kind can only be obtained if reliable formulation is available, based on results of careful theoretical and experimental studies of stress distribution. By the use of available technique and the simulation of the same conditions as those which exist in a ship's transverse bulkhead, we attempted to draw reliable conclusions concerning quantitative and qualitative characteristics of the stresses in the supports of a plate subjected to a concentrated co-planar compressive load.

One of the best techniques available is that of using the photo-elastic theory to determine stress patterns through isoclinics and isochromatic lines. This is the technique used in our experiments. By supporting the plate at the sides and bottom, we attempted to make conditions similar to a ship's transverse bulkhead. Furthermore, the simulation was improved by providing the plate with vertical centerline stiffeners for one part of the experiment.

The experimental work in this thesis was simplified a great deal by the fact that most of the apparatus needed was already available from previous work.⁽¹³⁾ Recommendations and results from this previous work were also considered.

At the request of the Society of Naval Architects and Marine Engineers the problem concerning the action of the stiffeners in distributing the deck loads into the sides and bottom of the vessel has been approached by other groups, utilizing rectangular flat plates of vari-

1. INTRODUCTION

However a structure is being designed all efforts are made to the designer toward a least weight solution that will fulfill the many requirements. A solution of this kind can only be obtained if reliable information is available, based on results of actual tests and experimental studies of stress distribution. If the use of available techniques and the utilization of the same solution as those which exist in a ship's structure is desired, it is necessary to have reliable conclusions regarding quantitative and qualitative characteristics of the stresses in the regions of a plate subjected to a concentrated or plane compressive load.

One of the best techniques available is that of using the photoelastic theory to determine stress patterns through isochromes and isoclinics lines. This is the technique used in our experiments. In preparing the plate of the sides and bottom, we attempted to make them similar to a ship's structure. Inasmuch as the simulation was improved by providing the plate with vertical centerline stiffeners for one part of the experiment.

The experimental work in this thesis was simplified a great deal by the fact that most of the equipment needed was already available from previous work. (1) Instruments and results from this previous work were also considered.

As the subject of the design of Naval Architects and Marine Engineers the problem concerning the stress of the stiffeners is of interest. The steel loads into the sides and bottom of the vessel are transmitted in other ways, utilizing rectangular flat plates of steel.

ous aspect ratios. The current practice in this matter is given by the Bureau of Ships which specifies that "stiffeners shall be arranged and designed so that when acting with a strip of bulkhead plating not exceeding sixty times the plating thickness they will be adequate to support that part of concentrated vertical loads which cannot be considered as being distributed to the bulkhead boundaries through shear in the bulkhead plating. The vertical load which is considered to be distributed to the boundaries by shear should be based upon a shear stress in the plating for one deck height (or where no deck is connected below the point of application of the load, then 7 feet) of about one-half the critical shear stress for the thickness of plating and size of panel in question." The check of the validity of such a specification was one of our goals in this thesis.

Several studies of plates subjected to normal and co-planar loads have been made. The investigation of failure by instability accounts for most of the literature in this field and the problem involving buckling loads of stiffened and unstiffened rectangular plates seems to be steadily approaching a satisfactory stage. Considerable work, both experimental and analytical, on buckling and failure of rectangular plates in compression⁽²⁰⁾, their behavior under the action of shearing forces⁽³⁾, and also, how they behave after buckling⁽⁷⁾, has been reported in the literature.

The stress distribution in flat plates at loads below critical have had less experimental attention and most investigation has been done analytically. Civil engineers have worked on the determination of stress distribution in deep beams⁽⁵⁾. This work is applicable to ship structure as well.

[illegible][illegible][illegible]

Photoelasticity has been used a great deal to determine stress distribution in beams. Several theories and statements have been checked by the use of this valuable tool. A quite remarkable reference to the use of this technique is the investigation of stresses in a rectangular bar by means of polarized light⁽⁸⁾ in 1912. The purpose of this study was to verify the results of Saint-Venant concerning the parabolic distribution of shear in a long bar of rectangular cross section at a distance from the points of loading.

The first attempt to investigate the stress distribution on a stiffened plate by the use of photoelasticity was presented, to the best of the writers' knowledge, by reference⁽¹³⁾ which limited the extent of the study to determination of the isoclinic pattern for three aspect ratios.

Several methods are available for determination of stresses. In reference⁽⁶⁾, for instance, a problem somewhat similar to ours was studied, namely, "the stress field of a plane plate reinforced by a longitudinal girder and subjected to tension in a direction parallel with the girder". Professor Hovgaard's method was to take the average value for shearing stresses between the girder and the plate at any section. He then obtained an expression for the relative displacement from the difference caused by these average stresses between plate and girder and the integral expression for the total elastic work in the system. From this, by the method of variation, the stresses were determined. In reference⁽⁶⁾, the actual instead of average stress was used by determining analytically the stress field. However, a continuously attached girder presented a quite involved mathematical analysis and caused the authors to replace the continuous attached girder by one

It is not possible to give a full and complete description of the work of the Commission in this field. The Commission has been very active in the study of the problems of the Negro people in the United States. It has held many public hearings and has received many suggestions from the public. It has also conducted many studies and has issued many reports. The Commission is very interested in the problems of the Negro people and is working hard to find ways to solve them. It is very grateful for the suggestions and help of the public.

The first report is devoted to the study of the
of the system, its structure and its functioning.
The second report is devoted to the study of the
of the system, its structure and its functioning.

[illegible]

attached to the plate at the ends only.

The method used in our work was the shear difference method⁽⁹⁾, which is based on the well-known differential equations of equilibrium in Cartesian coordinates. This method is considered to be the most powerful, direct and general of all available methods for the determination of normal stresses and deserves much wider use than it has received. It is relatively fast and simple and gives results of high accuracy. It is replacing all other methods for the determination of the separate normal or principal stresses across a section.*

*For a quick review on Photoelasticity Theory and on Shear-difference method see the Supplementary Introduction. For more detailed explanation refer to (19), chapter III and to (9), chapter VIII respectively.

...in the state of the world.

The second part is the first and the most important part.

which is based on the full-scale distribution of capital.

for the European countries. This second is connected to the first

part, which is based on the full-scale distribution of capital.

and the third part is the first and the most important part.

It is possible that the first and the most important part.

is connected to the first and the most important part.

which is based on the full-scale distribution of capital.

and the third part is the first and the most important part.

It is possible that the first and the most important part.

is connected to the first and the most important part.

and the third part is the first and the most important part.

It is possible that the first and the most important part.

is connected to the first and the most important part.

and the third part is the first and the most important part.

It is possible that the first and the most important part.

is connected to the first and the most important part.

and the third part is the first and the most important part.

It is possible that the first and the most important part.

is connected to the first and the most important part.

and the third part is the first and the most important part.

It is possible that the first and the most important part.

is connected to the first and the most important part.

and the third part is the first and the most important part.

II. PROCEDURE

The principal objective of this thesis was to determine the shear stress distribution on the side boundaries of a plate loaded in its own plane, and the variation of this stress distribution brought about by adding support on the bottom and finally by adding a centerline stiffener.

The photoelastic approach was used and calculations were made by use of the so-called Shear Difference Method. This method called for the determination of isoclinics and isochromatic lines on the model.

Two models of different materials were used. For the isochromatics, Catalin 61-893, a relatively sensitive material was used. A Plexiglass model was used to determine isoclinics because its low sensitivity made this determination easier. The plates were loaded on a special loading frame by a concentrated force on the centerline. A common load of 1630 lbs was used on all experiments because this load, we felt, would produce the number of lines needed for accuracy without critically straining the model. Four different conditions were examined; the plate supported on sides only, on sides and bottom, and each for the unstiffened and stiffened cases. The stiffeners were attached to the plate by using a special solvent, Penacolite Adhesive G-1124, manufactured by the Koppers Company, Inc., Pittsburgh. An attempt was made to obtain with strain gages the load transmitted by the stiffener. The method, however, did not prove successful.

The determination of the isoclinics was made by using the Plane Polariscopes Arrangement with white light. The isoclinics appeared as dark lines on the ground glass viewing screen. The load was varied until the best contrast was obtained, as isoclinics are independent of the load magni-

tude within the elastic limit.

The isoclinics were obtained at intervals of 10 degrees by simultaneously rotating counterclockwise both polariser and analyzer through that angle, and drawing them on tracing paper attached to the viewing screen.

The isochromatics were obtained by photography, using a leased Polaroid camera. Two different arrangements were used with monochromatic light. The Standard or Crossed Circular Polariscopes produced a dark field with the dark isochromatic lines corresponding to zero and integral orders of interference, while the Mixed Setup with the light field yielded dark isochromatics of half orders.

Because of the large size of the model relative to the lens system of the polariscope, it was not possible to photograph the whole model in a single picture. Pictures were taken of the sides for calculation purposes, and of the center to show the degree of alignment of loading.

With the data thus obtained, curves of direction of maximum principal stress and of the value of fringe orders were plotted. From these curves the shear stress distribution was obtained as shown in the Appendix. A more detailed discussion of the procedure can also be found in the Appendix.

(continued from page 60)

[illegible][illegible]

of the progress, and of the order to show the degree of alignment
model in a single instant. Figures were taken of the sides for the
end of the progress, it was not possible to photograph the whole
because of the large size of the model collected in the last year.

With the data thus obtained, curves of distribution of sediment grades along stream and of the values of stream velocity were plotted. From these curves the mean stream distribution was obtained as shown in the Appendix. A more detailed discussion of the procedure can also be found in the Appendix.

III. RESULTS

1. With the unstiffened plate supported at sides only and an applied load of 1650 pounds, the computed value of shear reaction on each side was 744 pounds.
2. With the unstiffened plate supported at sides and bottom and an applied load of 1650 pounds, the computed value of shear reaction on each side was 382 pounds.
3. With the stiffened plate supported at sides and bottom and an applied load of 1650 pounds, the computed value of shear reaction on each side was 451 pounds.
4. The distribution of shear stress over the plate edge for the three conditions of restraint is shown in Figure 1. The effect of the added bottom support was to displace the shear stress distribution curve toward the top of the plate.
5. It was found that the addition of the stiffener with the bottom support has the effect of increasing the side shear reaction.
6. Isochromatic and isoclinic patterns for the three conditions of restraint were obtained and are shown in the Appendix.
7. The attempt to use strain gages for obtaining the load taken by the stiffener proved inconclusive.

III. RESULTS

1. With the uniaxial plate supported at edges only and an applied load of 1650 pounds, the measured value of shear reaction on each side was 744 pounds.
2. With the uniaxial plate supported at edges and bottom and an applied load of 1650 pounds, the measured value of shear reaction on each side was 742 pounds.
3. With the uniaxial plate supported at edges and bottom and an applied load of 1650 pounds, the measured value of shear reaction on each side was 742 pounds.
4. The distribution of shear stress over the plate was for the three conditions of restraint is shown in Figure 1. The effect of the fixed bottom support was to displace the shear stress distribution curve toward the top of the plate.
5. It was found that the addition of the stiffener with the bottom support had the effect of increasing the side shear reaction.
6. Isoclinic and isochromatic patterns for the three conditions of restraint were obtained and are shown in the Appendix.
7. The attempt to use strain gages for obtaining the load taken by the stiffener proved inconclusive.

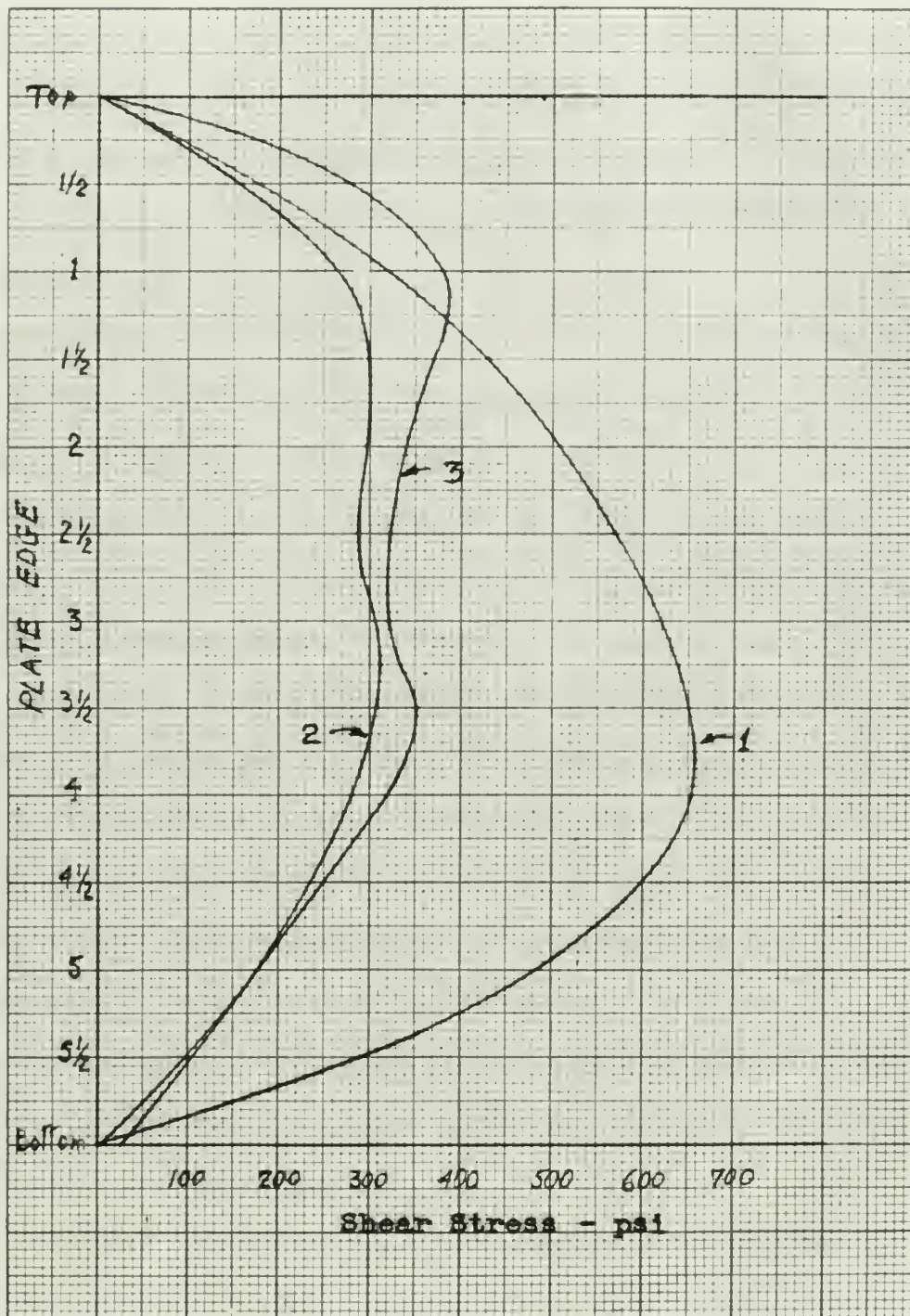


FIGURE I
SHEAR STRESS DISTRIBUTION

- 1 - Unstiffened plate supported at sides
- 2 - Unstiffened plate supported at sides and bottom
- 3 - Stiffened plate supported at sides and bottom

IV. DISCUSSION OF RESULTS

In order to evaluate the results of the experiment, it is necessary to consider the degree of accuracy of the methods used. This accuracy is dependent upon the precision of each step in the experimental procedure, namely, the measurement of the applied external load and the determination of the internal stress distribution.

The load cell and the Baldwin Indicator used to measure the external load applied through the load pin was estimated to have been accurate within 2%.

The determination of the stress distribution was dependent upon photo-elastic results and, therefore, its accuracy was limited by the difficulties encountered.

The fringe constant as determined from the tensile model test was 82.7. All references indicate a fringe value of 86.0 for the material used. This difference can be attributed either to experimental errors or to a difference in the material itself. This difference, however, will have no effect on the shapes of the computed shear stress distribution, as the same value is used throughout. The apparent accuracy of the shear difference method will be affected, since the value of the shear reaction at the plate sides is directly proportional to the value of the fringe constant.

The most inaccurate part of the experiment is believed to have been the determination of the isoclinic lines. These lines appeared as broad bands at some angles and as very faint lines at others, making the exact tracing of the pattern extremely difficult.

IV. DISCUSSION OF RESULTS

In order to evaluate the results of the experiment, it is necessary to consider the degree of accuracy of the methods used. This accuracy is dependent upon the precision of each step in the experimental process. First, namely, the measurement of the applied external load and the determination of the internal stress distribution. The load cell and the potentiometer used to measure the external load applied through the load pin was estimated to have been accurate within 1%. The determination of the stress distribution was dependent upon photo-elastic results and, therefore, the accuracy was limited by the difficulties encountered. The fringe constant as determined from the Isotrope model test was 85.7. All references indicate a fringe value of 85.0 for the material used. This difference may be attributed either to experimental errors or to a difference in the material itself. This difference, however, will have no effect on the shape of the computed shear stress distribution, as the same value is used throughout. The apparent accuracy of the shear differences noted will be affected, since the value of the shear constant at the plate ends is directly proportional to the value of the fringe constant. The most inaccurate part of the experiment is believed to have been the determination of the Isotrope lines. These lines appeared as broad bands of some angles and as very faint lines at others, making the exact drawing of the pattern extremely difficult.

Little difficulty was experienced in the determination of the isochromatics, however, exact centering of the load was never completely attained.

Edge effects present in the top and bottom edges of the plate changed slightly the isochromatic pattern in this vicinity and obscured some isotropic points, but should not have influenced the values of the fringe orders at the sides.

The use of two plates might have introduced some error because the side restraint might not have been exactly reproduced. It is felt, however, that this possible error was of minor order.

It was possible, in the case of the unstiffened plate supported at the sides only, to check the overall accuracy of the method, since the applied load should have equalled the total reaction. The applied load was measured as 1650 pounds, and the total reaction was computed as 1488 pounds. The overall experimental error, then, was 162 pounds or 9.8%.

By the addition of bottom support the total side reaction was reduced from 1488 pounds to 764 pounds, a reduction of 48.8% as should be expected.

With this same condition of restraint and the addition of a vertical centerline stiffener, the total shear reaction increased to 902 pounds, an 18.1% increase.

At first thought this might seem unreasonable because the addition of the stiffener would apparently increase the share of the load taken by the bottom. This, however, was not the case. The share of the load taken by the bottom is proportional to the deflection that the plate would have if there was no bottom support. The addition of the stiff-

little difficulty was experienced in the determination of the load characteristics, however, exact estimation of the load was never completely obtained.

When efforts were made in the form and position of the plate changed slightly the load characteristics in this study and showed some hysteresis, but should not have been noticed the values of the trials were as the same.

The use of the plate might have introduced some error because the side resistance might not have been exactly perpendicular. It is felt, however, that this possible error was of minor order.

It was possible, in the case of the uniaxial plate experiment as the plate only, to obtain the overall accuracy of the method, since the applied load should have equalled the total resistance. The applied load was measured as 1450 pounds, and the total resistance was reported as 1438 pounds. The overall experimental error, then, was 105 pounds or 9.8%.

By the addition of bottom support the total side reaction was reduced from 1450 pounds to 1400 pounds, a reduction of 48.8% or about 34% reduction. This was a reduction of resistance and the addition of a vertical compressive effort, the total shear reaction increased to 905 pounds, or 10.1% increase.

At first thought this might seem remarkable because the addition of the resistance would apparently increase the strain of the load along by the bottom. That, however, was not the case. The strain of the load along in the bottom is proportional to the deflection of the plate which gave it there was no bottom support. The addition of the side

ener naturally increased the bending stiffness of the plate, reducing the deflection that otherwise would have taken place in an unstiffened plate.

The shear stress distribution obtained for the unstiffened plate with side support was approximately parabolic in shape, with the maximum value occurring approximately at $.667 h$ (plate height) from the top.

When bottom support was added, the curve became flatter and was displaced toward the top. Two distinct humps of maximum shear stress were observed located at approximately $.250 h$ and $.583 h$ from the top.

Addition of the centerline stiffener with this same condition of restraint did not cause any marked change in the shape of the stress distribution curve. The increase in shear stress was more pronounced toward the top edge of the plate.

During the loading, the stiffened plate supported at the sides only, failed before the 1650 pound load used in the previous parts of the experiment was attained. It is believed that the failure can be attributed to the tri-axiality of stress developed at the stiffener connection. This is born out by the fact that the crack ran parallel to the stiffener weldment. It is interesting to note that the crack occurred in the plate itself indicating that Penacolite G-1124 provided a strong bond. Figure XIX shows a close-up of the plate after failure.

One other factor may or may not have affected our results. The plate was stress-relieved in the Laboratory oven to remove any effects of the first two parts of the experiment. During this stress relieving, a small area of the plate became plastic as a result of uneven heating in the oven. Upon rehardening, blotches appeared on the plate surface.

very similar to those of the plates, and the deflection of the plates was found to be in the same direction.

The shear stress distribution obtained in the deflected plates with the support was approximately parabolic in shape, with the maximum value occurring approximately at $y = 0.5$ (plate height) from the top. The bottom support was rigid, the shear stress was zero at the top. The deflected shape of the plates was stress was measured at approximately $y = 0.5$ and $y = 0.75$ from the top. A condition of the material was obtained with this same condition of restraint did not show any marked change in the shape of the stress distribution curve. The curves in shear stress were more pronounced about the top edge of the plate.

During the loading, the deflected plate was supported at the ends only, failed before the 1650 pound load was in the previous parts of the experiment was obtained. It is believed that the failure can be attributed to the end-conditions of stress developed in the stiffener connection. This is borne out by the fact that the stress was parallel to the stiffener web. It is interesting to note that the crack occurred in the plate itself indicating that the failure was not caused by a stress concentration. Figure 11 shows a close-up of the plate after failure.

One other factor may or may not have affected the results. The plate was stress-relieved in the laboratory oven at 200 degrees Fahrenheit for two hours at the beginning. During this stress relieving a small amount of the plate became plastic as a result of uneven heating in the oven. Upon reheating, distortion appeared on the plate surface.

The plate was reheated to 250° F and allowed to soak for a weekend. This apparently corrected these surface defects as the blotches all but disappeared.

The attempt to obtain the load transmitted through the stiffener was not successful because an improper technique was used. The strain gages indicated only local strain on the stiffener and this strain varied throughout its length. The total load, therefore, could not be evaluated.

This apparently contained below written details of the plot and all the circumstances.

The attempt to obtain the last mentioned through the British was not successful because an improved technique was used. The British also indicated only local results on the different and this was not verified throughout the length. The total load, therefore, could not be evaluated.

V. CONCLUSIONS

1. The Shear Difference Method, as used in this experiment, yields an overall accuracy within 10%.
2. The addition of a centerline stiffener reduces the part of the load taken by the bottom.
3. The addition of bottom support shows a definite trend in displacing the shear stress distribution curve toward the top edge of the plate. Also, this distribution curve becomes flatter and exhibits two distinct humps as compared with the parabolic shear distribution obtained with the side supports only.
4. The addition of a centerline stiffener does not appreciably affect the shape of this curve; however, the value of the total shear reaction, represented by the area under the curve, is increased.
5. The addition of a stiffener introduces tri-axiality of stress that may become critical at high loadings.
6. Penacolite G-1124 is an effective bonding adhesive in welding Catalin 61-893. This fact makes possible the use of this sensitive photo-elastic material in built-up models.
7. The technique used in evaluating the load transmitted through the stiffener proved unsatisfactory.

1. The three-dimensional method, as used in this experiment, provides an overall measure of the distribution of the load across the joint of the two plates.
2. The addition of a sanding surface between the two plates, as shown in the photograph, results in a more uniform distribution of the load across the joint of the two plates. Also, this distribution curve becomes flatter and wider.
3. The addition of a sanding surface above a flat surface in the joint of the two plates results in a more uniform distribution of the load across the joint of the two plates. Also, this distribution curve becomes flatter and wider.
4. The addition of a sanding surface does not appreciably affect the shape of the curve, however, the value of the total load is increased.
5. The addition of a different thickness of sanding material at high loadings, that may become critical at high loadings.
6. The addition of a sanding surface is an effective bonding adhesive in welding the two plates together.
7. The technique used in evaluating the load transmitted through the joint proved satisfactory.

VI. RECOMMENDATIONS

1. It is recommended that this photo-elastic study be continued and that emphasis be placed on:
 - a. Utilization of various aspect ratios so that its effect upon the shear stress distribution can be evaluated.
 - b. Utilization of more stiffeners symmetrically arranged to verify the trend displayed in this experiment.
2. Future studies should utilize two plates, namely, Catalin 61-893 for determination of isochromatics and a less sensitive material, such as Lucite, for determination of isoclinic lines.
3. An effort should be made to evaluate the load transmitted through the stiffeners. It is believed that this could be accomplished by utilization of several small strain gages mounted at various locations along the length of the stiffeners. In this way the stress distribution over the length of the stiffeners may be determined.

EXPERIMENTAL

1. It is recommended that this paper should be continued

and that the results be given as

a. The results of various experiments are given in

the following table and the results of the

analysis.

b. The results of the various experiments are

given in the following table and the results of the

analysis.

2. The results of the various experiments are given in

the following table and the results of the

analysis, given in the following table and the results of the

analysis. The results of the various experiments are

given in the following table and the results of the

analysis. The results of the various experiments are

given in the following table and the results of the

analysis. The results of the various experiments are

given in the following table.

VII APPENDIX

Introduction

The following is a summary of the main points of the report. It is intended to provide a general overview of the work done and the results obtained. The report is divided into several sections, each dealing with a different aspect of the problem. The first section deals with the general theory, the second with the experimental work, and the third with the results and conclusions. The fourth section deals with the discussion of the results and the fifth with the conclusions. The sixth section deals with the bibliography and the seventh with the index.

The first section deals with the general theory. It is divided into two parts. The first part deals with the general theory of the problem, and the second part deals with the specific theory of the problem. The second section deals with the experimental work. It is divided into two parts. The first part deals with the general experimental work, and the second part deals with the specific experimental work. The third section deals with the results and conclusions. It is divided into two parts. The first part deals with the general results and conclusions, and the second part deals with the specific results and conclusions. The fourth section deals with the discussion of the results. The fifth section deals with the conclusions. The sixth section deals with the bibliography. The seventh section deals with the index.

A. SUPPLEMENTARY INTRODUCTION

Elements of Photo-Elastic Theory

There are many stress analysis problems in which the deformation is essentially parallel to a plane. These are called two-dimensional problems. Plates of any shape but of constant thickness acted on by forces or couples in the plane of the plate may have such shapes that the stress distributions are very difficult to determine analytically and for such cases the photo-elastic method has proved very useful. In this method, models cut out of a plate of an isotropic transparent material such as glass, celluloid or bakelite are used. It is well known that under the action of stresses these materials become doubly refracting and, if a beam of polarized light is passed through a transparent model under stress, a picture with colored bands or with dark and light fringes may be obtained.

In the following explanation, we regard an ordinary beam of light as consisting of vibrations in all directions transverse to the direction of the ray. By passing the beam through a Nicol prism or a Polaroid disc or by reflecting it from a glass plate covered on one side with black paint, one obtains a more or less polarized beam of light in which transverse vibrations in a definite direction prevail. This is the kind of light used in investigating stress distributions in plates.

In Fig. XIV-A, "abcd" represents a transparent plate of uniform thickness and "O" is the point of intersection with the plate of a beam of polarized light perpendicular to the plate. Suppose that OA represents the plane of vibration of monochromatic light and that the length $OA = a$ represents the amplitude of this vibration. If the

vibration is considered to be simple harmonic, the displacements may be represented by the equation

$$s = a \cos pt \quad (1)$$

where p is proportional to the frequency of vibration, which depends on the color of the light.

Imagine now that the two principal stresses s_x and s_y , different in magnitude, are applied to the edges of the plate. Due to the difference in the stresses, the optical properties of the plate also become different in the two perpendicular directions. Let v_x and v_y denote the velocities of light in the planes OX and OY respectively. The simple vibration in plane OA is resolved into two components with amplitudes $OB = a \cos \alpha$ and $OC = a \sin \alpha$ in the planes OX and OY respectively, and the corresponding displacements are

$$x = a \cos \alpha \cos pt; \quad y = a \sin \alpha \cos pt. \quad (2)$$

If h is the thickness of the plate, the intervals of time necessary for the two component vibrations to cross the plate are

$$t_1 = \frac{h}{v_x} \quad \text{and} \quad t_2 = \frac{h}{v_y} \quad (3)$$

and vibrations (2) after crossing the plate are given by the equations:

$$x_1 = a \cos \alpha \cos p(t - t_1); \quad y_1 = a \sin \alpha \cos p(t - t_2). \quad (4)$$

These components have the phase difference $p(t_2 - t_1)$, due to the difference in velocities (v_x is assumed greater than v_y). Experiments show that the difference of these velocities of light is proportional to the difference in the principal stresses; that is, $v_x - v_y = c(s_x - s_y)$. Then, taking into account the fact that the changes of velocity of the light are very small and denoting by v the velocity of the light when the stresses are zero, we obtain the approximate equation

distortion is assumed to be negligible, the displacement may be represented by the equation

$$(1) \quad z = z_0 \cos pt$$

where z is proportional to the frequency of vibration, which depends on the value of the light.

Imagine now that the two principal stresses σ_1 and σ_2 , different in magnitude, are applied to the edges of the plate. Due to the difference in the stresses, the optical properties of the plate also become different in the two perpendicular directions. Let v_1 and v_2 denote the velocities of light in the plane of and of perpendicularity. The angles between the plane of vibration and the plane of and of perpendicularity

are α and β and the angles in the plane of and of perpendicularity, and the corresponding displacements are

$$(2) \quad x = a \cos \alpha \cos pt, \quad y = a \sin \alpha \cos pt, \quad z = z_0 \cos pt$$

If h is the thickness of the plate, the intervals of time necessary for the two component vibrations to cross the plate are

$$(3) \quad t_1 = \frac{h}{v_1} \quad \text{and} \quad t_2 = \frac{h}{v_2}$$

and relations (2) after inserting the plate are given by the equations

$$(4) \quad x = a \cos \alpha \cos p(t - t_1), \quad y = a \sin \alpha \cos p(t - t_2), \quad z = z_0 \cos pt$$

These equations have the same difference $(t_2 - t_1)$ due to the difference in velocities (v_1 is assumed greater than v_2). Experiments show that the difference of these velocities of light is proportional to the difference in the principal stresses; that is, $v_1 - v_2 = c(\sigma_1 - \sigma_2)$, then taking into account the fact that the velocity of light is very small and neglected by c the velocity of the light when the stresses are small, we obtain the approximate equations

$$t_2 - t_1 = \frac{h}{v_y} - \frac{h}{v_x} = \frac{h}{v_x v_y} (v_x - v_y) = \frac{h(v_x - v_y)}{v^2} = \frac{hc}{v^2} (s_x - s_y), \quad (5)$$

where c is a constant dependent on the physical properties of the material of the plate.

The difference of the two principal stresses can therefore be found by measuring the difference in phase of the two vibrations. This can be done by bringing them into interference in the same plane. For this purpose, another Nicol prism or Polaroid disc (called the analyser) is placed behind the plate in such a position as to permit the passage of vibrations in the plane "xm" perpendicular to the plane OM only. The components of the vibrations (4), which pass through the analyser, have the amplitudes $OB_1 = OB \sin \alpha = a \cos \alpha \sin \alpha = 1/2 a \sin 2\alpha$ and $OC_1 = OC \cos \alpha = a \sin \alpha \cos \alpha = 1/2 a \sin 2\alpha$. The resultant vibration in plane "xm" is

$$\begin{aligned} OC_1 \cos p(t - t_2) - OB_1 \cos p(t - t_1) &= \\ &= 1/2 a \sin 2\alpha \cos p(t - t_2) - 1/2 a \sin 2\alpha \cos p(t - t_1) = \\ &= (a \sin 2\alpha \sin p \frac{t_2 - t_1}{2}) \sin p(t - \frac{t_1 + t_2}{2}) \end{aligned} \quad (6)$$

This is a simple harmonic vibration whose amplitude is proportional to $\sin 1/2 p(t_2 - t_1)$; hence the intensity of the light is a function of the difference in phase $p(t_2 - t_1)$ or, from eq. (5) a function of the difference of the two principal stresses.

If the stresses s_x and s_y are equal, t_1 and t_2 are also equal and the amplitude of the resultant vibration (6) is zero, that is, the light is not transmitted at the point O and a dark spot occurs on the screen behind the analyser. There will be darkness also whenever the angle

$$1/2 p(t_2 - t_1) = n\pi \quad (7)$$

$$(1) \quad \left(\frac{1}{\sqrt{1-\beta^2}} - \frac{1}{\sqrt{1-\beta'^2}} \right) \frac{1}{\sqrt{1-\beta^2}} = \frac{1}{\sqrt{1-\beta^2}} \left(\frac{1}{\sqrt{1-\beta'^2}} - \frac{1}{\sqrt{1-\beta^2}} \right) + \frac{1}{\sqrt{1-\beta^2}} \left(\frac{1}{\sqrt{1-\beta'^2}} - \frac{1}{\sqrt{1-\beta^2}} \right)$$

where β is a constant dependent on the physical properties of the medium.

Let us now consider the case of two waves.

The difference of the two physical quantities can therefore be found by considering the difference in phase of the two vibrations. This can be done by writing the two vibrations in the same phase. For this purpose, suppose that the two vibrations are of the same frequency. Let the first vibration be $y = a \sin \alpha x + b \cos \alpha x$ and the second be $y' = a' \sin \alpha' x + b' \cos \alpha' x$. The resultant vibration is given by

$$y + y' = (a \sin \alpha x + b \cos \alpha x) + (a' \sin \alpha' x + b' \cos \alpha' x)$$

$$= (a \sin \alpha x + a' \sin \alpha' x) + (b \cos \alpha x + b' \cos \alpha' x)$$

$$= (a \sin \alpha x + a' \sin \alpha' x) \cos \alpha x + (b \cos \alpha x + b' \cos \alpha' x) \sin \alpha x$$

(2)

This is a simple harmonic vibration whose amplitude is proportional to the sum of the amplitudes of the two vibrations. Since the intensity of the light is a function of the amplitude, it follows that the intensity of the light is a function of the distance of the two vibrations. (3) or, from eq. (2), a function of the distance of the two vibrations.

If the distances α and α' are equal, α and α' are also equal and the amplitude of the resultant vibration (3) is equal to the sum of the amplitudes of the two vibrations. If the distances α and α' are not equal, the amplitude of the resultant vibration (3) is less than the sum of the amplitudes of the two vibrations. There will be a minimum when the two vibrations are out of phase.

$$(3) \quad y + y' = (a \sin \alpha x + a' \sin \alpha' x) \cos \alpha x + (b \cos \alpha x + b' \cos \alpha' x) \sin \alpha x$$

where n is an integer. The maximum intensity of light will be obtained when the difference in principal stresses is such that

$$1/2 p(t_2 - t_1) = n\pi + \frac{\pi}{2}$$

By substituting $t_2 - t_1$ from eq. (4) into eq. (7) and then setting

$$\frac{2\pi v^2}{phc} = K_d \quad (8)$$

one gets

$$s_x - s_y = \frac{2\pi v^2}{phc} \quad n = n K_d \quad (9)$$

denoting that there will be darkness whenever the difference of the principal stresses becomes equal to an integral multiple of K_d .

To determine the value of K_d , let us replace the element "abcd" (Fig. XIV-A) under biaxial stress by a strip of similar material under simple tension ($s_y = 0$). By gradually increasing the tensile stress s_x , we obtain a dark picture of the strip on the screen each time eq.(9) is fulfilled. In this manner we can establish experimentally, for a given material of given thickness, the stress corresponding to the interval between two consecutive dark pictures of the specimen. With this information, we can determine the total stress in a strip under tension by counting the number of intervals between the consecutive dark images occurring during the gradual loading of the specimen.

With K_d known, the photo-elastic method gives the difference, $s_x - s_y$, of the two principal stresses as discussed in the second paragraph above. It also gives the maximum shearing stress directly because the maximum shear stress is equal to $1/2 (s_x - s_y)$. Hence eq.(9) may be written in the form

$$(s_s)_{\max} = nK \quad (10)$$

where α is an arbitrary constant. The solution obtained in (1) will be obtained when the following is indicated: $\alpha = 0$.

$$y = \frac{1}{2} (1 + \sqrt{1 - 4x})$$

By substituting $y = \frac{1}{2} (1 + \sqrt{1 - 4x})$ in (1), (2) and (3) we obtain

$$(4) \quad \frac{dy}{dx} = \frac{1}{2} (1 - \sqrt{1 - 4x})$$

and

$$(5) \quad \frac{d^2y}{dx^2} = \frac{1}{2} (1 - \sqrt{1 - 4x})$$

Substituting these into the differential equation, we obtain the identity $0 = 0$.

To determine the value of y , we replace the constant α by

$$(6) \quad y = \frac{1}{2} (1 + \sqrt{1 - 4x})$$

which satisfies (1), (2) and (3). It is easily verified that this function is a solution of the differential equation.

It is also easy to see that the function $y = \frac{1}{2} (1 - \sqrt{1 - 4x})$ is a solution of the differential equation.

between two consecutive dark fringes of the spectrum. With this in

mind, we can calculate the total energy in a single wave packet

by assuming the value of λ obtained from the previous calculation. The energy density of the radiation is

$$u = \frac{1}{2} \epsilon_0 E^2$$

where E is the electric field strength. The energy density in the wave packet is

$$u = \frac{1}{2} \epsilon_0 E^2$$

may be written in the form

$$(7) \quad u = \frac{1}{2} \epsilon_0 E^2$$

where $K = K_d/2$. So it may also be stated that there is darkness whenever $(s_s)_{\max}$ becomes equal to an integral multiple of K .

Each of the dark fringes in a stressed specimen is the locus of points where the maximum shearing stress or the difference of the principal stresses is constant. By watching the specimen while the load is applied gradually, we may see how the number of dark fringes increases with increase of load. The new ones always appear at the top and the bottom of the beam and gradually move toward the neutral plane so that the fringes become more and more closely packed. The stress at any point is then obtained by counting the number of fringes which pass over the point.

Having introduced some of the basic theory underlying the photo-elastic method of stress analysis, let us consider in more detail the photo-elastic equipment used for quantitative work. The Polariscopes, as the apparatus is called, consists of the elements shown in Fig. XIV-C. The source of light may be an incandescent lamp giving white light or a mercury vapor arc lamp giving monochromatic light. The former will give a pattern of brilliant bands of different colors or hues each one representing a constant value for the difference between the two principal stresses. These bands have been designated by the name "isochromatics". The alternate bright and dark lines formed in monochromatic light are also isochromatics (though sometimes called interference "fringes") and are distinguished from one another according to the value of n . consequently, they are often referred to as the isochromatic of zero, first, second order of interference, and so on. The water cooler removes heat energy from the light rays so that the Canada balsam in

about 2-3 mm. It is not clear whether this is the same as the

over (a) but the point is an interesting addition of it.

That of the dark brown is a somewhat different in the point of

points where the surface is covered with the thickness of the
principal structure is somewhat. By looking at the structure with the
load is applied gradually, we may see the nature of the change
increased with increase of load. The two main points appear at the
top and the bottom of the beam and gradually move toward the center
plane so that the change becomes more and more clearly marked. The
upper at any point in time obtained by counting the number of changes
which pass over the point.

Having introduced some of the facts about the structure of the

elastic nature of the material. Let us consider in more detail the

photo-elastic equipment used for quantitative work. The photograph

as the apparatus is called, consists of the elements shown in Fig. 1-2.

The source of light may be an incandescent lamp giving white light or

a mercury vapor arc lamp giving monochromatic light. The former will

give a pattern of brilliant bands of different colors or lines when the

producing a constant value for the difference between the two plates

of the thickness. These colors have been designated by the name "isochromes"

isochromes. The isochromes which are first formed in the

white light are also isochromes (though sometimes called interference

"fringes") and are distinguished from one another according to the value

of a constant, that are often referred to as the "order" of the

zero, first, second order of interference, and so on. The order of

remains constant from the light rays as they are changed within the

the Nicol prisms will not melt. The purpose of the quarter-wave plates will shortly be discussed.

Returning to a consideration of eq. (6), we see that the amplitude of vibration of light passing through the analyzer is proportional also to $\sin 2\alpha$, where α is the angle between the plane of polarization and the plane of one of the principal stresses (Fig. XIV-A). If these two planes coincide, $\sin 2\alpha$ is zero and we obtain a dark spot on the screen. Hence in examining a stressed transparent model in polarized light, we observe not merely the dark fringes discussed before but also dark lines (isoclinics) connecting the points at which one of the principal stresses coincides with the plane of polarization. By rotating both Nicol prisms and marking the dark lines on the image of the stressed plate for various directions of the plane of polarization, we obtain the system of so-called isoclinic lines which join together points with the same directions of principal stresses. Having these lines, we can draw the lines which are tangential at each point to the principal axes of stress. These latter lines are called "the trajectories of the principal stresses". Thus the directions of the principal stresses at each point of the plate can be obtained experimentally.

These isoclinics may be distinguished from the stress fringes by rotating both Nicol prisms alike. The stress fringes do not shift position but the isoclinics do. Usually, however, the isoclinics are removed entirely by inserting quarter-wave plates as shown in Fig. XIV-C. A quarter-wave plate resolves a transverse vibration into two components at right angles to each other; this plate is made of a doubly refracting material such as mica and with such a thickness that it retards one of these components of vibration a quarter-wave length more than the other.

the wave plates will not melt. The purpose of the quarter-wave plates
will be explained.

Returning to a consideration of eq. (6), we see that the direction
of vibration of light passing through the analyzer is proportional also
to $\sin \alpha$, where α is the angle between the plane of polarization and
the plane of one of the principal stresses (Fig. XIV-4). If these two
planes coincide, $\sin \alpha$ is also $\sin \alpha$ and we obtain a dark spot on the screen.

Since in examining a stressed transparent model in polarized light, we
observe not merely the dark fringes discussed before but also dark lines
(isoclinics) connecting the points at which one of the principal stresses
coincides with the plane of polarization. By rotating both glass plates
and rotating the dark lines on the image of the stressed plate for which
one direction of the plane of polarization, we obtain the system of so-
called isoclinic lines which join together points at which the two direc-
tions of principal stresses. Having these lines, we can then find the
which are tangential at each point to the principal axes of stress.

These latter lines are called 'the trajectories of the principal stresses'.
Thus the directions of the principal stresses at each point of
the plate can be obtained experimentally.

These isoclinics may be distinguished from the stress fringes by
rotating both glass plates like. The stress fringes do not shift, but
also not the isoclinics do. Usually, however, the isoclinics are re-
solved optically by inserting quarter-wave plates as shown in Fig. XIV-5.
A quarter-wave plate converts a circular vibration into two compo-

nents at right angles to each other; this plate is made of a doubly refracting
material such as mica and with even a thickness that is several microns.
These components of vibration a quarter-wave length more than the other,

The first quarter-wave plate in Fig. XIV-C with its axis at 45° to the initial plane of vibration of the polarized light, produces two component displacements, one parallel to its axis and one perpendicular thereto. These displacements vary exactly in the same manner as the coordinates "u" and "v" of point A moving uniformly on the circumference of a circle (Fig. XIV-B) and for this reason the light emerging from the first quarter-wave plate is said to be circularly polarized. The second quarter-wave plate in Fig. XIV-C restores the plane polarized light if no stressed model is present. An equation similar to eq. (6) can be derived for the vibration of a beam of light after passage through the polariscope including quarter-wave plates and stressed model. The resulting equation differs from eq. (6) in that the term $\sin 2\alpha$ has disappeared from the amplitude portion of the expression, showing that the amplitude of the resulting vibration is independent of α and consequently no isoclinic lines are present.

The use of monochromatic light is preferred by most workers for obtaining stress patterns because the dark fringes photograph much more readily and are easier to use than the colored patterns. White light is better for obtaining isoclinics because they show up as dark fringes against a colored background.

The Shear Difference Method

The magnitude of the shear stress (s_s) at any point on any arbitrary straight line across a plane is given by the expression

$$(s_s) = \frac{(s_x - s_y)}{2} \sin 2\theta'$$

where θ' is the acute angle measured from the normal to the arbitrary straight line to the direction of the algebraically maximum principal stress s_x .

The first quarter-wave plate in Fig. IV-5, with the axis of X in the initial plane of vibration of the polarized light, produces the required displacement, and parallel to the axis and one perpendicular to the axis. These displacements vary exactly in the same manner as the cosine of πy and πz of point A moving uniformly on the circumference of a circle (Fig. IV-5) and for this reason the light emerging from the first quarter-wave plate is said to be circularly polarized. The second quarter-wave plate in Fig. IV-5 restores the light polarized light if no external field is present. An equation similar to eq. (8) can be derived for the vibration of a beam of light after passing through the polarizer retaining quarter-wave plates and crossed plates. The resulting equation differs from eq. (8) in that the term $\cos \alpha$ has disappeared from the right-hand portion of the expression, leaving just the magnitude of the resulting vibration is independent of α and consequently no focusing takes place.

The use of rotatable light is prevented by the fact that the rotating plates become the dark regions in the photograph when the light is not in the center of the colored portion. This light is better for obtaining resolution because they show up as dark regions against a colored background.

The First Quarter-Wave Plate

The magnitude of the wave stress (σ) at any point on the vibrating standing film within a plate is given by the expression

$$\sigma = \frac{2E\epsilon}{\lambda} \sin \frac{2\pi y}{\lambda} \sin \frac{2\pi z}{\lambda}$$

where E is the elastic modulus of the material of the plate, λ is the wavelength of the vibration of the plate, and y and z are the coordinates of the plate.

The photo-elastic method provides the necessary and sufficient data to evaluate (s_s) . The stress patterns give $(s_x - s_y)$, and the isoclinics give the directions of the principal stresses, i. e., the angle θ' . The numerical values of the shear stress (s_s) can thus be easily calculated at all points.

The above definition of θ' is very convenient because its direction will be the same as the direction of the shear stress s_s .

The following steps outline the procedure for applying the shear-difference method in our work:

1. Draw curves of n and θ' for the edge in question.
2. Determine the direction of s_s by inspection of the θ' curve and by knowing the direction of principal stresses at a particular point along the edge (intersection with upper edge in compression is an example).
3. Compute shear stresses at a sufficient number of points of the edge to permit the plotting of the shear stress curve (s_s) . This computation is made by the use of the expression

$$s_s = \frac{s_x - s_y}{2} \sin 2\theta' = nK \sin 2\theta'$$

where values of n and θ' are available from step 1 and K is the fringe constant for the transparent material used and determined as explained previously.

4. A static check is provided by measuring the area under the shear curve with a planimeter or by Simpson's rule, giving an average shear stress. The total shear across the edge is then given by

$$V = (s_s)_{\text{mean}} \cdot A$$

where A is the area of the edge section. This value of V is then compared against the actual V .

The photo-elastic method provides the necessary and sufficient data to evaluate (σ_1) . The stress intensity factor (K_I) and the residual stress (σ_r) of the specimen are known, i. e., the angle θ . The theoretical value of the stress (σ_1) can then be easily calculated at all points.

The above definition of θ is very convenient because the direction will be the same as the direction of the shear stress σ_{xy} . The following steps outline the procedure for applying the photo-elastic method in our work:

1. First order of θ and ϕ for the case in question.
2. Determine the direction of σ_1 by inspection of the θ curves and by finding the direction of principal stresses at a particular point θ (intersection with $\theta = 0$ in the expression is an example).
3. Compute shear stresses at a sufficient number of points of the edge to permit the plotting of the shear stress curve (σ_{xy}) . This computation is made by the use of the expression

$$\sigma_{xy} = \frac{\sigma_1 - \sigma_2}{2} \sin 2\theta = \frac{\sigma_1 - \sigma_2}{2} \sin 2\phi$$

where values of θ and ϕ are available from step 1 and 2 in the figure. The shear stress σ_{xy} and the direction θ are determined as explained previously.

4. A stress curve is provided by measuring the area under the shear stress curve with a planimeter or by Simpson's rule, giving an average stress value. The total shear stress σ_{xy} is then given by

$$\sigma_{xy} = \frac{1}{A} \int \sigma_{xy} dA$$

where A is the area of the edge studied. The value of σ_{xy} is then compared with the value of σ_{xy} from step 3.

B. DETAILS OF PROCEDURE

Polariscope

All of the elements of the polariscope required by this thesis were available in the Experimental Stress Analysis Laboratory. A general view of the Laboratory setup can be seen in Figure XVI, and a schematic diagram of the polariscope is enclosed as Figure XIV.

The polariscope was equipped with sources of both white and monochromatic light which could be interchanged quickly. White light was produced by an incandescent bulb of 500 watts capacity. Monochromatic light was obtained from a d-c mercury-arc. Wratten filters, 58 and 77-A, were used to mask out radiations other than the "green" line. This filter also aided in obtaining sharply defined fringes in the isochromatic diagrams.

The polarizer and analyzer were Nicol prisms and because of their small diameter, a lens system was required to produce a field of sufficient size for studying the model.

Quarter-wave plates were mounted on the same stands as the polarizer and analyzer and were readily accessible and easily removable.

All of the above equipment was mounted on an optical bench. This bench was rigid and the upper surface was free from any projecting brackets or supports so as to permit the continuous uninterrupted sliding of the lenses and prisms resting upon it. The optical bench consisted of two independent parts with the load frame between them. The two sections were aligned and securely fastened in place.

The part before the load frame held the light source, water cell, filter and auxiliary lens, polarizer, quarter-wave plate, and the first collimating lens. The second part supported the second collimating lens,

Observations

All of the elements of the polarographic apparatus of this design were available in the Department of Agriculture laboratory. A new half size of the laboratory setup was used in Figure VII, and a somewhat different of the polarographic is enclosed in Figure XIV. The polarographic was equipped with sources of both white and monochromatic light which could be interchanged rapidly. White light was produced by an incandescent bulb of 100 watts capacity. Monochromatic light was obtained from a low temperature, heated filament, 50 and 75-watt used to make two variations when the "Green" line, 540 mμ, for also used in obtaining sharply defined images in the microprojector.

The polarograph and analyzer were placed on a base of heavy metal. A lens system was required to project a beam of white light also for studying the model.

Quartz-ray plates were mounted on the base stands on the polarograph and analyzer and were readily accessible and easily removable. All of the above equipment was mounted on an optical bench. This bench was rigid and the upper surface was flat and perfectly level. In order to support the system the condenser and microscope objectives of the lenses and prism resting upon it. The optical system consisted of two independent parts with the lens between them. The two sections were aligned and accurately focused in place.

The part before the lens was held the light source, water cell, filter and analyzing lens, polarizer, quartz-ray plate, and the first collimating lens. The second part supported the second collimating lens,

second quarter-wave plate, the analyzer, and the camera.

The camera was set on two runners, as was all the equipment on the bench. These runners and the individual supports of each piece of equipment provided for longitudinal as well as vertical movement. Thumb screws could be used to lock the supports in place both longitudinally and vertically. Another set of thumb screws permitted slight transverse adjustment of the polariscope units.

The lens and shutter system of camera were removed, leaving only the bellows. Viewing screens and a polaroid camera were easily inserted at the after end of these bellows providing excellent mobility in focusing and aligning the equipment before photographs were taken.

Although all the equipment required was available, the polariscope had to be set to give the best image for our particular problem.

The first step in the setting of the polariscope was to align the polarizer, analyzer, and all lenses so that their centers lay on one line parallel to the long axis of the optical bench which was checked and found to be horizontal.

The next step was to make sure that the field on the screen was of uniform intensity and well defined. To this end the polarizer was set to give a circularly polarized field and the analyzer to give a bright image on the screen. This called for a mixed setup. The lamp and other elements were adjusted so that the screen field was circular with a sharp outline, and free from color or black blotches.

The elements of the polariscope were then locked into position and these positions were marked along the side of the bench with masking tape.

Load Frame

It is obvious that a suitable straining machine is essential for

second quarter-wave plate, the analyzer, and the screen.

The camera was set on two stands, as was all the equipment on the bench. These stands and the individual supports of each piece of equipment

were provided for adjustment as well as vertical movement. These

adjustments could be made to lock the supports in place both longitudinally and vertically. Another set of three screws provided slight transverse

adjustment of the polarizing units.

The lens and shutter system of camera were removed, leaving only the bellows. Viewing screen and a polaroid camera were easily inserted

at the other end of these bellows providing excellent stability in focus and adjusting the exposure before photographs were taken.

Although all the equipment required was available, the polarizing

had to be set to give the best image for our particular problem.

The first step in the setting of the polarizing was to align the

polarizer, analyzer, and all lenses so that their centers lay on the

line parallel to the long axis of the optical bench which was checked

and found to be horizontal.

The next step was to make sure that the field on the screen was of

uniform intensity and well defined. In this way the polarizer was set

to give a horizontally polarized field and the analyzer to give a bright

image on the screen. This method for a second check. The lens and camera

elements were adjusted so that the narrow field was observed with a

sharp outline, and then from above or below position.

The elements of the polarimeter were then locked into position and

these positions were marked along the side of the bench after setting was

completed.

It is obvious that a complete attention machine is essential for

photoelastic studies. The problems in a photoelastic laboratory are different from those of a material testing laboratory, and the equipment, therefore, must also be different.

The devices used to apply external loads to a model vary a great deal depending upon individual requirements of special models.

For this thesis a load frame belonging to the Ships Structure Laboratory of the Massachusetts Institute of Technology was used.

A minute description and detailed construction plan for this load frame is found in reference 13.

The load frame is built of aluminum, and its parts are shown schematically in the Appendix.

It is made essentially of a $3/4$ inch thick base plate, to which are attached four vertical posts. These posts are made of two opposing channels placed in such a way that a transverse loading bar can work between them.

At the top the vertical posts are attached to a supporting horizontal bar.

The inner posts have holes drilled $1\ 1/2$ inches apart to permit the clamping of the model.

The outer posts have $3/4$ inch diameter holes spaced 2 inches apart to permit vertical adjustment of the pivot point of the transverse loading bar.

The pivot pin bears on two bronze bushings placed in matching holes of the outer posts.

The load pin is connected to a sliding attachment on the transverse loading bar.

The first part of the book is devoted to a description of the anatomy of the human eye. The author discusses the various parts of the eye, including the cornea, iris, lens, and retina, and explains how they work together to form an image. He also discusses the various diseases of the eye and the methods of treatment. The second part of the book is devoted to a description of the anatomy of the human ear. The author discusses the various parts of the ear, including the eardrum, ossicles, and cochlea, and explains how they work together to hear sound. He also discusses the various diseases of the ear and the methods of treatment. The third part of the book is devoted to a description of the anatomy of the human nose. The author discusses the various parts of the nose, including the nostrils, nasal cavity, and sinuses, and explains how they work together to breathe. He also discusses the various diseases of the nose and the methods of treatment. The fourth part of the book is devoted to a description of the anatomy of the human mouth. The author discusses the various parts of the mouth, including the lips, tongue, and throat, and explains how they work together to eat and speak. He also discusses the various diseases of the mouth and the methods of treatment. The fifth part of the book is devoted to a description of the anatomy of the human throat. The author discusses the various parts of the throat, including the larynx, trachea, and bronchi, and explains how they work together to breathe. He also discusses the various diseases of the throat and the methods of treatment. The sixth part of the book is devoted to a description of the anatomy of the human lungs. The author discusses the various parts of the lungs, including the bronchi, alveoli, and pleura, and explains how they work together to breathe. He also discusses the various diseases of the lungs and the methods of treatment. The seventh part of the book is devoted to a description of the anatomy of the human heart. The author discusses the various parts of the heart, including the atria, ventricles, and valves, and explains how they work together to pump blood. He also discusses the various diseases of the heart and the methods of treatment. The eighth part of the book is devoted to a description of the anatomy of the human blood vessels. The author discusses the various parts of the blood vessels, including the arteries, veins, and capillaries, and explains how they work together to transport blood. He also discusses the various diseases of the blood vessels and the methods of treatment. The ninth part of the book is devoted to a description of the anatomy of the human nervous system. The author discusses the various parts of the nervous system, including the brain, spinal cord, and nerves, and explains how they work together to control the body. He also discusses the various diseases of the nervous system and the methods of treatment. The tenth part of the book is devoted to a description of the anatomy of the human reproductive system. The author discusses the various parts of the reproductive system, including the testes, ovaries, and uterus, and explains how they work together to produce offspring. He also discusses the various diseases of the reproductive system and the methods of treatment. The book is written in a clear and concise style, and is suitable for use as a textbook or a reference work. It is a valuable addition to any library of medical books.

The whole frame is supported by horizontal roller bearings on a steel I beam. A cross feeding mechanism moves the load frame along the I beam providing for lateral positioning of the model in its own plane.

The beam rests on a steel table having vertical movement. This table is part of the equipment of the Stress Analysis Laboratory.

Thus, both lateral and vertical movement of the load frame can be accomplished easily.

Some modifications were made to suit the particular needs of this experiment.

One of the fundamental requirements for photoelastic work is flexibility and smoothness in loading. In order to determine the general formation of the stress pattern and the fringe orders at a particular point, it is necessary to watch the growing or changing stress pattern under gradually changing loads.

The original frame included a water tank to achieve this varying load. Several authors recommend this weight hydraulic system for smoothest loading.

It was decided, however, that the tank would introduce complications not only because of the required water connections but also because the high loads needed in this problem would cause the deflections of the horizontal bar to become excessive, introducing misalignment in the loading of the plate.

Instead, a hydraulic jack, borrowed from the Ship Structure Laboratory was placed directly over the sliding support of the load pin. The other support for the jack was provided by the upper transverse beam of the load frame.

The following is a description of the apparatus used in the experiments. It consists of a rectangular tank, 100 cm long, 50 cm wide, and 100 cm high, filled with water. A vertical rod, 100 cm long, is attached to the top of the tank, and a horizontal rod, 50 cm long, is attached to the side of the tank. A weight, 100 g, is attached to the end of the horizontal rod. The weight is submerged in the water, and the vertical rod is moved up and down, causing the weight to move up and down. The distance between the top of the tank and the weight is measured, and the time taken for the weight to move a certain distance is recorded. The experiment is repeated for different weights and different distances, and the results are plotted on a graph. The graph shows that the time taken for the weight to move a certain distance is proportional to the square root of the distance. This is the expected result for motion with constant acceleration.

In this manner a higher load could be achieved without the errors introduced by the bending of the bar, and the load could be changed quickly to suit the immediate needs of the experiment. This setup worked pretty well even though some difficulties were encountered in the alignment of the jack itself. By observing the symmetry of the isochromatic pattern obtained, it was always possible to center the applied load.

The vertical channels had to be changed to accommodate the model. The size of the latter was limited by the width of the plate, 12 inches, furnished by the Catalin Corporation. Allowing a margin for the clamping of the model, the distance between the vertical posts had to be reduced to $9 \frac{3}{4}$ inches.

This was easily accomplished by boring and threading new holes in the base plate.

This work was done by the Machine Shop of the Institute.

The load was applied to the model by a $1/2$ inch diameter cylindrical load pin, acting on the plate through a $3/16$ inch diameter load pin. To avoid excessive stress concentration and local plastic deformation, the $3/16$ inch pin did not make direct contact with the plate. It rested on a small aluminum bar of $3/4$ inch length and of the same thickness as the plate.

In transmitting the load from the small aluminum bar to the plate itself, a thin piece of cardboard with the same dimensions as the bar was used.

This cardboard was used to eliminate a common difficulty present in photo-elastic work, that of the improper distribution of load.

In this manner a higher load could be applied without the danger

introduced by the bending of the bar, and the load could be applied

entirely so with the knowledge of the magnitude of the load.

When the load was applied the deflection was measured by

the alignment of the bar itself. By observing the position of the

load relative to the bar, it was always possible to make the

applied load.

The vertical distance was to be applied to the bar in the

The distance of the bar was fixed by the value of the load, it being

fixed by the distance between the points of support. The distance

of the bar, the distance between the points of support had to be

fixed to 2 1/4 inches.

This was usually accomplished by having the distance between the

the bar plate.

This work was done in the Machine Shop of the Institute.

The load was applied to the bar by a 1/2 inch diameter rod

and load pin, acting on the plate through a 1/2 inch diameter load pin

to avoid excessive stress concentration and local plastic deformation.

The 3/16 inch pin did not make direct contact with the plate. It was

on a small diameter bar of 3/16 inch diameter and of the same material

as the plate.

In removing the load from the small distance pin to the plate

itself, a thin piece of cardboard with the same dimensions as the bar

was used.

This cardboard was used to eliminate a possible difficulty in

in photo-graphic work. Part of the specimen distribution of load.

In order for the fringes to be continuous and sharply defined, stresses and strains must be two-dimensional. Otherwise, breaks and discontinuities appear in the stress pattern.

To eliminate such discontinuities, the loads must be uniformly distributed across the thickness of the model by means of some equalizer. The simplest equalizer is a piece of cardboard.

The load pin comprises a built-in load cell. This load cell is composed of four SR-4 type A-7 strain gages.

Two of them are placed on opposite sides of the load pin and two are attached to pieces of aluminum bar. The latter act as dummy gages for temperature compensation.

These gages were connected such that they form the arms of a Wheatstone bridge as shown in the Appendix. This setup eliminated any indication of bending and gave a true indication of the axial force through the pin.

These gages were tested for shorts or discontinuities with a potentiometer and were found to be in good operating condition.

The next step was to calibrate the load cell.

For this purpose the load pin was put in series with a Standard Baldwin Load Cell belonging to the Stress Analysis Laboratory.

The load pin gages and its dummies were connected to an SR-4 Baldwin Indicator with a gage factor setting of 1.92.

A calibration curve plotted, indicated a response of 1.058 in/in per pound.

In order to get even numbers, which are easier to work with, a new gage factor setting which would provide an indication of 1.00 in/in per pound was found.

[illegible]

Using the general equation for strain gages indicators:

$$\text{true} \times \text{G.F. true} = \text{indicated} \times \text{GF indicated},$$

we obtain

$$\text{GF in} = \frac{t \times \text{GFt}}{\text{in}} \quad \text{Eq (11)}$$

$$\text{GF in} = \frac{1.038 \times 1.92}{1.00} = 2.03$$

Therefore, a gage factor of 2.03 was used in order to obtain the desired response.

A new calibration run was made using this value for checking purposes.

The calibration curve is shown in the Appendix.

Before each run a zero reading was made and the value of any load could be easily obtained by using the conversion factor of 1.00 in/in per pound.

The precision on the load measurement was dependent upon the minimum resolution of the strain indicator, which was estimated to be about 2.00 in/in.

Photographic equipment

The polariscope arrangement of the Photoelastic Laboratory is that of transmission type, using Nicol prism. This polariscope setup is well adapted for photographic work.

Accurate loading of the model is of prime importance in attaining good results. First the model used was roughly symmetrically loaded, then the loading was adjusted until a symmetrical pattern was obtained.

The sharpness and general appearance of the photoelastic stress pattern was greatly improved by coating the surfaces of the model with

Using the general equation for strain rate sensitivity

$$\sigma = K \dot{\epsilon}^n \quad \text{where } n = 3.7, K = 1.0 \times 10^{-4} \text{ (in units of } \text{lb/in}^2 \cdot \text{s})$$

we obtain

$$\sigma = 1.0 \times 10^{-4} \dot{\epsilon}^{3.7} \quad (1)$$

$$\dot{\epsilon} = \frac{\sigma}{1.0 \times 10^{-4}}^{1/3.7} = 1.03 \times 10^3 \text{ s}^{-1}$$

Therefore, a grain length of 2.0 μ was used in order to obtain the same

strain rate.

A new calculation was made using this value for the grain length

to give

The calculated curve is shown in the Appendix.

Below each are a curve resulting from the value of grain length

could be easily obtained by using the same value of grain length of 2.0 μ

per grain.

The prediction on the load measurement was dependent upon the grain

size prediction of the strain rate. This was estimated to be about

2.0 μ in.

Experimental results

The experimental arrangement in the Instron is shown in Fig. 1

of Instron type, using strain gages. The Instron type is well

suited for this type of work.

Results of the work in the Instron are shown in Fig. 2

good results. The Instron was used with a specially designed fixture

from the Instron was adjusted with a specially designed fixture was obtained.

The Instron was used with a specially designed fixture was obtained.

Results are shown in Fig. 3 of the Instron work.

a light clear oil, Mufol, and then wiping them clean. This served the double purpose of removing finger marks and filling in many tiny scratches.

The actual photographic work was greatly simplified because of the facilities provided on the polariscope setup. The frame of the ground glass viewing screen on the outside part of the bellows is interchangeable with two other frames. One contains a Land Polaroid camera, and another contains a smaller ground glass viewing screen, the same size as the polaroid print and with the same focal distance as the camera itself. The procedure was to focus the picture on this screen, then, exchange this frame for the one containing the camera. The photograph was then taken with no difficulty.

The advantages of the Land Polaroid camera for this type of experiment cannot be over emphasized. To have a picture developed and ready to be analyzed in 60 seconds is a tremendous help when time is at a premium.

As the shutter had been removed from the camera, an improvised shutter had to be devised.

The time of exposure required to photograph a stress pattern depends on many factors, such as intensity of light source, magnification of the image, emulsion speed of the photographic film and the transparency of the model.

The improvised shutter was made of two pieces of cardboard rotated manually in front of the light beam. The first trials with the high speed film Polaroid Type 44 were not satisfactory.

In order to make exposure time less critical, we used the slower Polaroid film Type 41. The results were then very satisfactory as can

a light green oil, which had been lying there since. This served the
double purpose of covering their work and filling in any gaps
between.

The actual photographing took place exactly opposite to the
the facilities provided at the photographic station. The frame of the
ground glass viewing screen on the outside part of the bellows is in-
comparable with the other frame. One contains a lead plate and
one, and another contains a smaller ground glass viewing screen, the
same size as the bellows part and with the same focal distance as the
other lens. The projection was to form the picture on this screen,
which, according to the focus for the lens, would be the same. The photo-
graph was taken with no difficulty.

The advantage of the lead plate is that the size of the
picture could be very regulated. It has a picture developed in
ready to be enlarged to 60 inches is a tremendous help when time is at
a premium.

In the winter had been removed from the camera, an important
element had to be added.

The size of exposure required in photographing a given pattern de-
pends on many factors, such as intensity of light source, position
of the image, position of the photographic film and the trans-
parency of the model.

The photograph contains the side of the object of interest exposed
usually in front of the light source. The third subject will be the
spot film photograph type of which has explanatory.

In order to make exposure the lens critical, we used the same
bellows film type A. The results were then very satisfactory in the

be seen by the photographs obtained. Because of the large size of the model it was not possible to photograph the whole model at one time.

The procedure was to take a picture showing the side boundary and another showing the center part of the model.

Three different pictures were taken for each condition investigated: two of the sides, one with the circular dark field arrangement showing the lines of integral order and another with the circular light field showing the half orders. The third photograph was taken with the dark field arrangement at the center to show the degree of symmetry attained in the loading.

Preparation of Models

The photoelastic material selected for a given model is always the result of a compromise to secure the largest number of desirable properties with the fewest undesirable characteristics. For our experiments Catalin 61-893 (formerly Bakelite BT-61-893) seemed to be the best choice. It has good strength properties, a relatively high modulus of elasticity, and, optically, is moderately sensitive to stress. For stresses below 4000 psi the creep effect is negligible in a period of a few hours. The machining properties are reasonably good, and its time-edge effect is not excessive.

The two Catalin plates ordered from the Catalin Corporation of New York arrived in the unfinished and unpolished state. Several unexpected steps then became necessary before the actual experimental work could be started.

Sketches of the desired tensile model and stiffeners^e were supplied to the Institute Machine Shop. The Shop machined the model and stiffeners to the specifications of these sketches. The tensile model was

1. The first step is to identify the problem or question that needs to be answered. This involves understanding the context and the specific requirements of the task.

The government will take a further step to help the building

© 1999 by John Wiley & Sons, Inc.

—continued on inside back cover

[illegible]

ALL INFORMATION CONTAINED HEREIN IS UNCLASSIFIED EXCEPT WHERE SHOWN OTHERWISE

[Faint, illegible text at the bottom of the page]

scholars to reach out and work with business and the managerial field and

... ..

1992

and the fact that the system is not a simple linear system.

Figure 1. Schematic diagram of the experimental setup. The subject is seated in a chair and views the screen through a mirror. The screen displays the target and the starting position of the hand. The hand is moved from the starting position to the target position. The distance between the starting position and the target position is the reach distance. The distance between the starting position and the target position is the reach distance.

... ..

© 1999 John Wiley & Sons, Inc. CCC 0890-6895/99/010000-01

Individuals To Inform: All individuals ≥ 65 years of age, except those aged 65 and 66

100-443887-100

THE UNIVERSITY OF CHICAGO PRESS

ni jantia arborescens est, sed, dum fructum suum immaturum habet, non

For environmental scientists and policy-makers alike, the following are key messages:

with *Journal of the American Academy of Child and Adolescent Psychiatry* 41:10 (October 2002): 1233-1240.

Our estimations indicate that the effect of the 1990s on the growth rate of the economy is positive and significant.

Patrons may use the fee ~~to~~ ^{to} attend for up to 50 minutes.

to the University of Illinois. The first meeting of the group was held

For citation purposes only, please refer to the journal website for the full article.

then polished to a smooth and clear finish. All polishing was done on the polishing wheels of the Experimental Stress Laboratory using a solution of aluminum oxide and water as the abrasive. The wheel itself was covered with black Italian velvet.

The plate model was also polished in the above manner. The plate, however, presented added complications as it was noticeably warped. An attempt to remove the curvature by placing the plate in oil, heating to 240°F, soaking at that temperature for a few hours, and then cooling slowly, proved unsuccessful. A second attempt was made by grinding the corners of the plate and heating to 240°F in the small insulated furnace of the Experimental Stress Analysis Laboratory. After several cycles of prolonged heating and gradual cooling with the plate resting on a flat piece of glass, the curvature was removed. Subsequent examination under polarized light showed the model to be stress free.

Horizontal and vertical reference lines spaced one inch apart were etched on the surface of the plate. Finally, a coat of Mufol, a light mineral oil, was applied to the surface of the plate to remove any finger marks and fill in any small scratches.

The stiffeners, because they would not be examined photoelastically, did not require any fine polishing. One SR4 Type A-7 strain gage was mounted on each side of the stiffeners with Duco cement. After the gages were mounted, the stiffeners were placed to dry in the furnace at 80°F for about 24 hours.

Once the first parts of the experiment were over, that is those with the plate in the unstiffened condition, the stiffeners were welded to the models. Penacolite G-1124 was used as the binding adhesive. First the Penacolite was spread on the plate along the vertical centerline

then polished to a smooth and clean finish. All polishing was done on the polishing wheels of the Experimental Stress Laboratory using a solution of aluminum oxide and water as the abrasive. The wheel itself was covered with black Italian velvet.

The plate model was also polished in the above manner. The plate, however, presented added complications as it was noticeably warped. In attempt to remove the curvature by placing the plate in oil, heating to 240°F , soaking at that temperature for a few hours, and then cooling slowly, proved unsuccessful. A second attempt was made by grinding the corners of the plate and heating to 240°F in the well insulated furnace of the Experimental Stress Analysis Laboratory. After several cycles of prolonged heating and gradual cooling with the plate resting on a flat piece of glass, the curvature was removed. Subsequent examination under polarized light showed the model to be stress free.

Horizontal and vertical reference lines spaced one inch apart were etched on the surface of the plate. Finally, a coat of Wipol, a light mineral oil, was applied to the surface of the plate to remove any film that might get into any small scratches.

The stiffeners, because they could not be examined photographically, did not require any film polishing. One G-1 type 1-7 strain gage was mounted on each side of the stiffeners with Duco cement. After the gages were mounted, the stiffeners were placed in dry ice for about 24 hours at 80°F for about 24 hours.

Once the first parts of the experiment were over, that is those with the plate in the unstressed condition, the stiffeners were welded to the models. Pennacott's G-114 was used as the bonding adhesive. First the Pennacott's was spread on the plate along the vertical centerline

where the stiffener was to be welded, and also along the edge of the stiffener itself. After a ten minute wait the two were joined in their proper positions. Pressure was then applied and maintained overnight. Two stiffeners were used, one on each side of the plate. The stiffeners were made of Catalin 61-893 and were each 6" x 1/2" x 1/4" in size. A more detailed description of the welding procedure is given in reference 16.

Determination of Fringe Constant

The fringe constant is really a stress-optic constant for the material. It is a property of the material and may vary from batch to batch, as slight differences in curing time and method may easily occur. As the stress magnitude at any point in a photoelastic model is directly proportional to the fringe constant as well as the fringe order, an accurate determination of the former is quite necessary for satisfactory results.

For this reason a tensile model was made and the fringe constant determined by a tensile test. The model was placed in a loading frame as shown in Figure XVIII. The circular polariscope with the dark field arrangement was used and a tensile load was gradually applied to the model. The load was measured by a Baldwin SR-4 load cell connected to a load cell analyzer. At the start a no-load reading was taken. As the load was increased, isochromatic lines appeared as a dark shadow over the entire shank of the model. This shadow appeared, became dark, and disappeared in cycles as the load was gradually increased. The darkest color of each cycle indicated an integral order of interference, and strain readings were taken as each order appeared. After six orders were observed, the load was gradually reduced and readings were taken as

where the stiffener was to be welded, and also along the edge of the stiffener itself. After a few minutes with the two parts joined in their proper position, the pressure was then applied and maintained overnight. Two stiffeners were used, one on each side of the plate. The stiffeners were made of Detail (1-8) and were each $1\frac{1}{2} \times 1\frac{1}{4}$ in size. A more detailed description of the welding procedure is given in Section 10.

Determination of Fringe Constant

The fringe constant is really a stress-optic constant for the material. It is a property of the material and may vary from plate to plate, as slight differences in curing time and method may easily occur. As the stress increases at any point in a photoelastic model is directly proportional to the fringe constant as well as the fringe order, so accurate determination of the former is quite necessary for satisfactory results.

For this reason a tensile model was made and the fringe constant determined by a tensile test. The model was placed in a loading frame as shown in Figure XVII. The circular photoelasticity with the dark field arrangement was used and a tensile load was gradually applied to the model. The load was measured by a Baldwin beam cell connected to a load cell analyzer. At the start a no-load reading was taken. As the load was increased, the photoelastic lines appeared as a dark shadow over the entire length of the model. This shadow appeared, became dark, and disappeared in cycles as the load was gradually increased. The faint color of the model followed an inverted order of interference, and strain readings were taken as each cycle appeared. When six cycles were observed, the load was gradually reduced and readings were taken as

the orders reappeared. This procedure was repeated and a graph of strain reading in μ -in/in versus order of interference, Figure XIII. was plotted. The slope of this curve was determined as 310 μ -in/in/order. Using the formula $F.C. = \frac{1}{b} \frac{\Delta p}{\Delta n}$ equation (12) (where $\frac{\Delta p}{\Delta n}$ is the slope of the curve with 1 lb equal to 10 μ -in/in and b equal to the width of the tensile model in this case .375 inches), the fringe constant was determined to be 82.7 lb/in -order with monochromatic light of wave length 5461 \AA .

Detailed Procedure of Experimental Work

Once these preliminary items were disposed of, the actual experimental work was started.

The unstiffened Catalin plate was placed in the load frame with its bottom edge two inches above the base plate of the frame. The plate was temporarily supported by two rectangular steel bars each one inch thick and placed one on top of the other. Two thin steel plates with flat edges were used on each end of the plate. By placing one of these plates between each side of Catalin plate and the channels of the load frame, better clamping was obtained than would have been possible had only the rounded edge channels been used. The screws were tightened by hand and the model centered between the edge supports. The clamping was then completed by tightening the screws with wrenches. The screws were tightened from the center of each edge outward toward the top and bottom. Approximately equal pressure was put on each screw in an attempt to make the clamping as uniform as possible. The two steel bars beneath the plate were then removed.

The cardboard equalizer and the small aluminum load bar were then centered on the top edge of the plate with the load pin centered hori-

centally across them. The loading arm was then lowered about its pivot point until the vertical load pin on the sliding attachment rested on the horizontal load pin. With the plate clamped two inches above the base plate of load frame, the load arm of the frame was nearly horizontal which made it easier to obtain a symmetrical load distribution.

The hydraulic jack was placed between the sliding attachment of the load arm and the upper cross member of the load frame. Thin wooden blocks were used on each end of the jack to aid in evenly distributing the load. The jack, sliding attachment, and load pin were centered as closely as possible. Pressure was applied to the jack and the load on the model gradually increased until several isochromatic lines appeared on the viewing screen.

Usually the load was not made symmetrical on the first attempt. In these cases, the pressure was released and minor adjustments made to the position of the jack, sliding attachment, and load pin. The pressure was reapplied and the whole procedure repeated until a symmetrical distribution of load was observed. A load of 1650 pounds, enough to give sufficient lines for calculation purposes and still not overstress the plate, was applied.

At this point the large viewing screen was removed and the smaller one inserted. This small screen displayed an image of exactly the same size as that which could be reproduced by the polaroid camera. In addition, if the image was focused sharply on the screen, the same focus would be sharp for the camera. The viewing screen and camera were not large enough to reproduce the image of the whole plate. Separate settings and photographs had to be made for the center and the side.

The model image was centered on the viewing screen by adjusting the

exactly same point. The loading was then lowered about the given
 point until the vertical load was in the sliding position and so
 the horizontal load was. With the plate placed two inches above the
 base plate of the frame, the load was at the same vertical position.
 For this case it was to obtain a symmetrical load distribution.
 The hydraulic load was placed between the sliding adjustment of
 the load and the upper cross member of the load frame. This means
 the load was used as a guide and the load is in evenly distributed
 the load. The load, sliding adjustment, and load pin were connected as
 closely as possible. Pressure was applied to the load and the load was
 the load gradually increased until several load increments were applied
 on the sliding member.
 Usually the load was not quite symmetrical on the sliding member. In
 these cases, the pressure was reduced and some adjustment was made to the
 position of the load, sliding adjustment, and load pin. The pressure
 was reapplied and the whole procedure repeated until a symmetrical dis-
 tribution of load was obtained. A load of 1500 pounds was applied in five
 increments from the calibration program and still not symmetrical the
 plate, was applied.
 At this point the large sliding member was removed and the loading
 was inserted. This small member displaced on a scale of weight the same
 as that which would be represented by the balance beam. It will
 then, if the large was removed directly on the balance, the same force
 would be shown for the balance. The sliding member was removed and
 large enough to represent the size of the small plate. The small plate
 then was inserted and the balance was set for the same and the slide.
 The small plate was centered on the sliding member for adjusting the

supporting table and cross feed mechanism of the load frame. The image was sharply focused on the viewing screen, and the screen replaced by the polaroid camera. The load was rechecked and the photograph taken.

In taking the photographs, the exposure time had to be judged by trial and error since the shutter and lens system of the camera had been removed to fit the camera into the bellows of the polariscope. The correct exposure time was achieved by using two cardboard sheets. The two sheets were held flat against each other forming a triangular slit between them. One sheet was held in front of the quarterwave plate and analyzer while the light excluding slide of the camera was removed. The sheets were then rotated smartly across the light beam until the second cardboard covered the quarter wave plate opening. The slide was then replaced across the camera mouth. After a sixty second wait the picture was removed from the camera.

The load frame was then moved with the cross feed mechanism until the desired image of the plate side appeared on the viewing screen which was now substituted for the camera. The side which gave the clearest image was selected and the above procedure repeated to give a photograph of the integral orders at the side. A 1650 pound load was used for all photographs of isochromatics to allow a better comparison between photographs.

The half order isoclinics were obtained by rotating the polarizer 90° giving a circular polariscope with the light field. These half order isoclinics allowed more points to be plotted on the fringe order curve which was used in the shear difference method computations.

[illegible]

1. The first of these is the fact that the
2. The second is the fact that the
3. The third is the fact that the
4. The fourth is the fact that the
5. The fifth is the fact that the
6. The sixth is the fact that the
7. The seventh is the fact that the
8. The eighth is the fact that the
9. The ninth is the fact that the
10. The tenth is the fact that the

[illegible][illegible]

After the load was released, the equipment was removed and the screws holding the plate were loosened. The Catalin plate was then removed, and the Plexiglass plate was placed in the frame in the same manner.

As isoclinic lines do not vary with load within the elastic limit, the load which gave the clearest pattern of isoclinic lines was applied to the model.

The quarter wave plates were removed and white light through the Wratten filter was used.

The large viewing screen was inserted and focused since tracing paper rather than photographs were used to reproduce the isoclinics.

The symmetry of load was attained by checking that the 0° isoclinic lay along the vertical centerline of the plate. After the load was centered the load frame was moved to the clearest side. Tracing paper was taped over the screen and the reference lines of the plate image were drawn.

The polarizer and analyzer were simultaneously rotated 10° counterclockwise and the 10° isoclinic lines were traced on the paper and labeled. The polarizer and analyzer were rotated 10° more, and so on until a full cycle, 90° was recorded. Intermediate angles were recorded when they appeared necessary for the clarity of the pattern.

This entire procedure for obtaining the isochromatics and the isoclinic lines was repeated for the unstiffened plates supported on the bottom as well as the sides, and for the stiffened plates in both support conditions.

The procedure was varied slightly when bottom support was added. A piece of cardboard was placed between the bottom edge of the plate

After the load was released, the magnet was removed and the

current feeding the plate was terminated. The carbon plate was then re-

moved, and the electrode plate was placed in the frame in the usual

manner.

In assembling the lines to the very end of the electrode plate,

the load which gave the element potential of localized lines was applied

to the plate, and the current was allowed to flow for a few minutes.

The current was then removed and the plate was allowed to

remain for one hour.

The large electrode plate was removed and the carbon plate was

placed in the frame and the current was allowed to flow for a few

minutes. The current was then removed and the plate was allowed to

remain for one hour. After the load

was removed the load frame was moved to the adjacent side. The

current was then applied over the carbon and the electrode plate of the plate

was removed.

The electrode plate was then removed and the carbon plate was

placed in the frame and the current was allowed to flow for a few

minutes. The current was then removed and the plate was allowed to

remain for one hour. The electrode plate was then removed and the

carbon plate was placed in the frame and the current was allowed to

flow for a few minutes. The current was then removed and the

plate was allowed to remain for one hour. The electrode plate was

then removed and the carbon plate was placed in the frame and the

current was allowed to flow for a few

minutes. The current was then removed and the plate was allowed to

remain for one hour. The electrode plate was then removed and the

and the base plate of the load frame. While the screws which clamped the sides of the plate were being tightened, light pressure was applied to the plate forcing it against the frame base plate. These two steps were taken in an attempt to insure even distribution of support across the bottom of the plate. The support table for the load frame had to be raised two inches to center the model in the light beam, and the load arm pivot point had to be dropped two inches to permit the load arm to remain nearly horizontal when the load pin rested on the top edge of the plate.

The strain gages attached to the plate stiffener and the dummy gages for temperature compensation were connected forming the arms of a Wheatstone Bridge. A zero reading and subsequent readings as the load was gradually increased to 1650 pounds were recorded. These readings were plotted as strain on stiffener versus applied load as shown in Figure XX.

During the determination of the isochromatics of the stiffened plate with side clamping only, the Catalin plate failed before the 1650 pound load was reached. A loud snap was heard and the load was immediately removed. The plate was examined and a large crack running up from the bottom edge, parallel to the stiffener, was observed. This failure is shown in Figure XIX.

and the base of the lead frame. While the specimen was being
the edges of the plate were being supported, light pressure was applied
to the plate forcing it against the lower base plate. These two steps
were taken in an attempt to insure even distribution of support across
the bottom of the plate. The support table for the lead frame had to
be raised and locked to make the metal in the light form and the lead
and glass parts had to be moved two inches to permit the lead to be
remains nearly horizontal when the lead was worked on the top edge of
the plate.

The strain gages attached to the finite section and the lower glass
for temperature compensation were connected leading the ends of a short
glass bridge. A wire solder and subsequent readings on the lead and
gradually increased to 1000 pounds were recorded. These readings were
plotted as strain on a strain versus weight load as shown in Figure III.
During the preparation of the instrumentation of the specimen
plate with side clamping only, the bottom plate failed before the 1000
pounds load was reached. A lead strip was placed and the lead was locked
later removed. The plate was examined and a large crack running up
from the bottom edge, parallel to the specimen, was observed. This
failure is shown in Figure III.

APPENDIX C
DATA AND CALCULATIONS

THE

CONSTITUTION

TABLE I

UNSTIFFENED PLATE
Supported at sides only

<u>Station</u>	<u>Order</u>	<u>θ</u>	<u>$\sin 2\theta$</u>	<u>τ</u>
0 (Top)	.80	90°	0	0
1/2	1.23	50.0	.985	179
1	2.15	32.5	.906	287
1 1/2	3.60	27.0	.809	430
2	4.50	25.0	.766	508
2 1/2	5.01	25.0	.766	566
3	5.20	26.5	.799	612
3 1/2	5.20	29.0	.848	650
4	4.89	32.5	.906	654
4 1/2	4.15	37.0	.961	587
5	3.38	37.5	.966	483
5 1/2	2.50	27.0	.809	298
6 (Bottom)	2.00	0	0	0

Applied load at center of plate - 1650 lbs.

Computed shear force on each edge - 744 lbs.

TABLE I

STANDARD PLATE
values in the 1000 series

λ	σ_{λ}	ρ_{λ}	μ_{λ}	ν_{λ}
0	0	0.00	0.00	0 (Top)
100	0.00	0.00	0.00	1
200	0.00	0.00	0.00	2
300	0.00	0.00	0.00	3
400	0.00	0.00	0.00	4
500	0.00	0.00	0.00	5
600	0.00	0.00	0.00	6
700	0.00	0.00	0.00	7
800	0.00	0.00	0.00	8
900	0.00	0.00	0.00	9
1000	0	0	0.00	10 (Bottom)

Applied load at center of plate - 1000 lbs.
Applied load at each edge - 100 lbs.

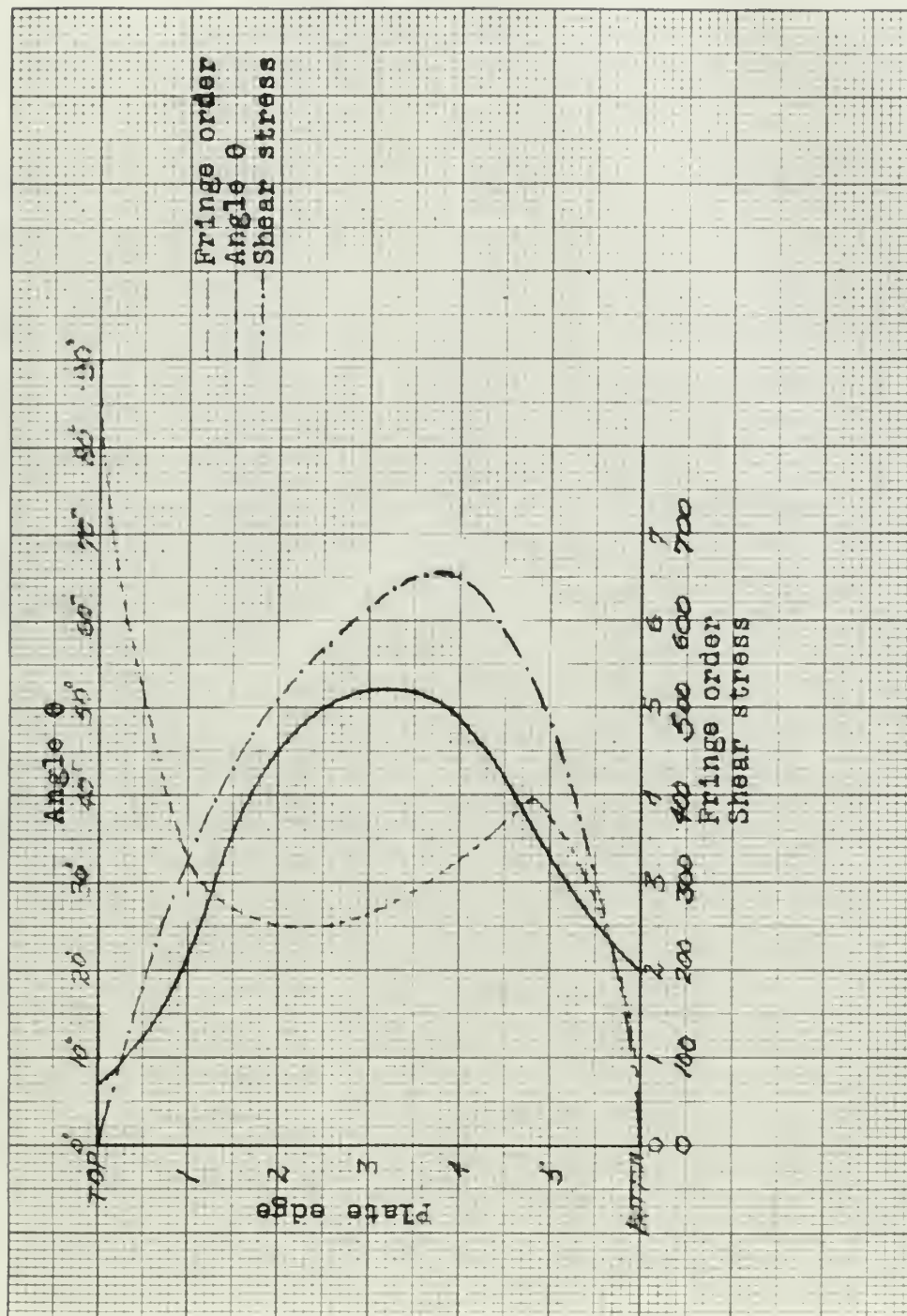


FIGURE II
UNSTIFFENED PLATE
Supported at sides only
Load 1650 lbs.

TABLE II

UNSTIFFENED PLATE
Supported at sides and bottom

<u>Station</u>	<u>Order</u>	<u>θ</u>	<u>$\sin 2\theta$</u>	<u>τ</u>
0 (Top)	0	90	0	0
1/2	1.1	51	.978	158.5
1	2.1	29	.848	262.0
1 1/2	2.9	22	.695	298.0
2	3.1	20	.643	294.0
2 1/2	2.9	21	.670	286.0
3	2.7	25	.766	303.0
3 1/2	2.4	30	.865	306.5
4	2.0	36	.951	280.0
4 1/2	1.6	41	.990	233.5
5	1.2	46	.999	177.0
5 1/2	.7	50	.985	101.8
6 (Bottom)	.2	55	.940	27.7

Applied load at center of plate - 1650 lbs.

Computed shear force on each edge - 382 lbs.

TABLE II

UNITED STATES
NAVY DEPARTMENT
BUREAU OF NAVAL ARCHITECTURE

Location	Order	W	AS, ft	W
0 (Top)	0	90	0	0
1/2	1.1	82	879.	1.0
1	2.1	75	848.	2.0
1 1/2	3.1	68	822.	3.0
2	4.1	60	800.	4.0
2 1/2	5.1	52	779.	5.0
3	6.1	45	760.	6.0
3 1/2	7.1	38	742.	7.0
4	8.1	30	725.	8.0
4 1/2	9.1	22	709.	9.0
5	10.1	15	694.	10.0
5 1/2	11.1	8	679.	11.0
6 (Bottom)	12.1	0	664.	12.0

Applied load at center of plate - 100 lbs.
Applied shear force on each edge - 100 lbs.

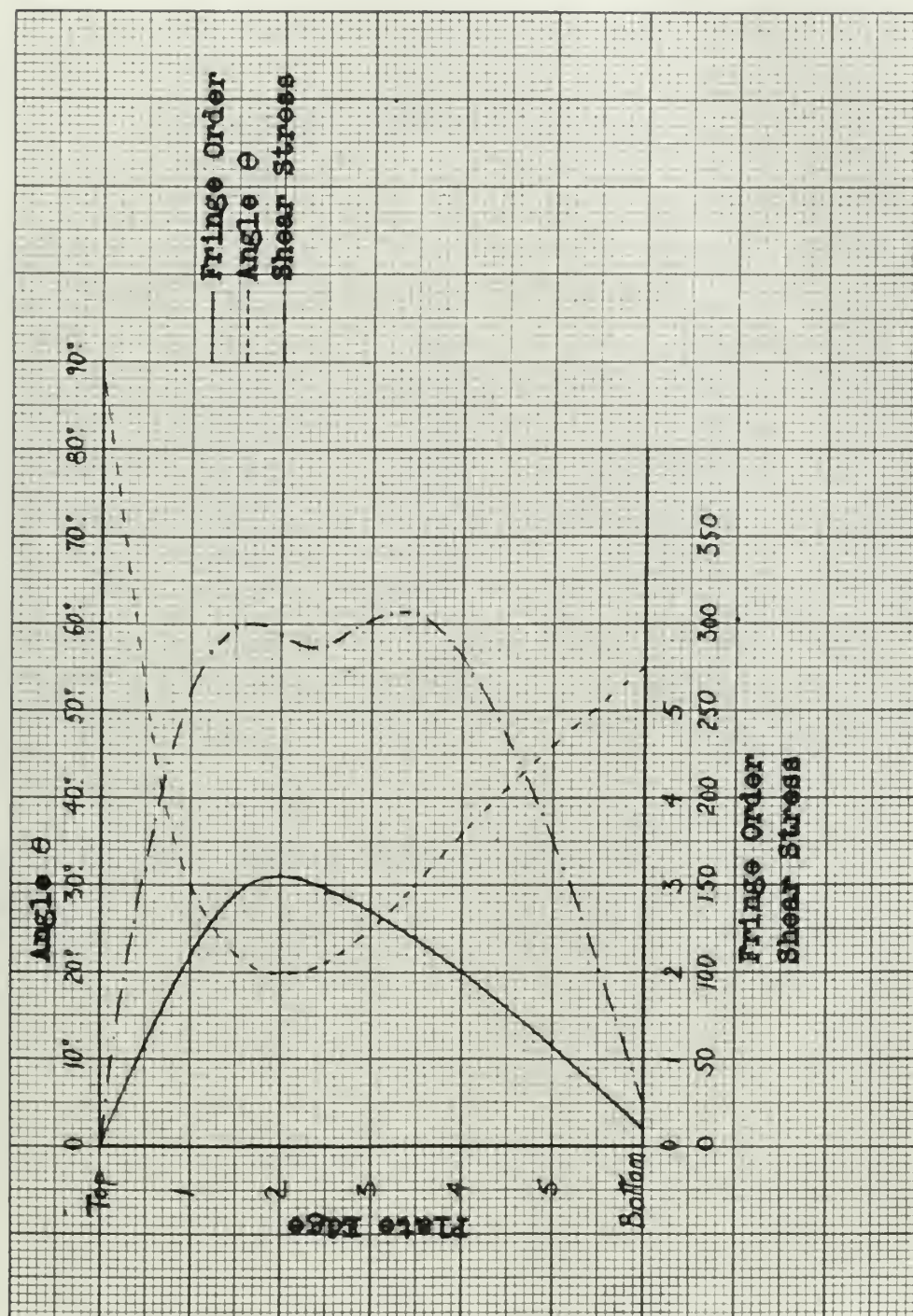


FIGURE III
 UNSTIFFENED PLATE
 Supported at sides and bottom
 Load 1650 lbs

TABLE III
STIFFENED PLATE
 Supported at sides and bottom

<u>Station</u>	<u>Order</u>	<u>θ</u>	<u>$\sin 2\theta$</u>	<u>τ</u>
0 (Top)	1.60	90°	0	0
1 2	1.95	59.5	.945	272
1	2.65	48	.970	379
1 1 2	3.27	25	.766	370
2	3.58	20	.643	340
2 1 2	3.65	18.5	.602	322
3	3.30	20.5	.656	320
3 1 2	2.72	30.5	.875	351
4	2.20	39.5	.982	319
4 1 2	1.60	46	.999	236
5	1.20	51	.978	173
5 1 2	0.70	54.5	.945	98
6 (Bottom)	0.00	56.5	.921	0

Applied load at center of plate - 1650 lbs.

Computed shear force on each edge - 451 lbs.

TABLE III
 REINFORCED PLATE
 Supported at sides and bottom

Station	Center	$\frac{1}{4}$	Side	$\frac{1}{8}$
0 (Top)	1.40	90.0	0	0
1 2	1.75	99.2	.945	575
1	2.05	98	.970	379
1 2	2.27	95	.966	360
2	2.48	90	.943	340
2 1 2	2.65	78.5	.905	322
3	2.70	70.2	.856	300
3 1 2	2.75	60.5	.812	281
4	2.70	49.5	.961	279
4 1 2	1.40	45	.999	236
5	1.20	21	.918	173
5 1 2	0.70	24.5	.945	98
6 (Bottom)	0.00	26.5	.951	0

Applied load at center of plate - 1650 lbs.
 Computed shear force on each edge - 451 lbs.

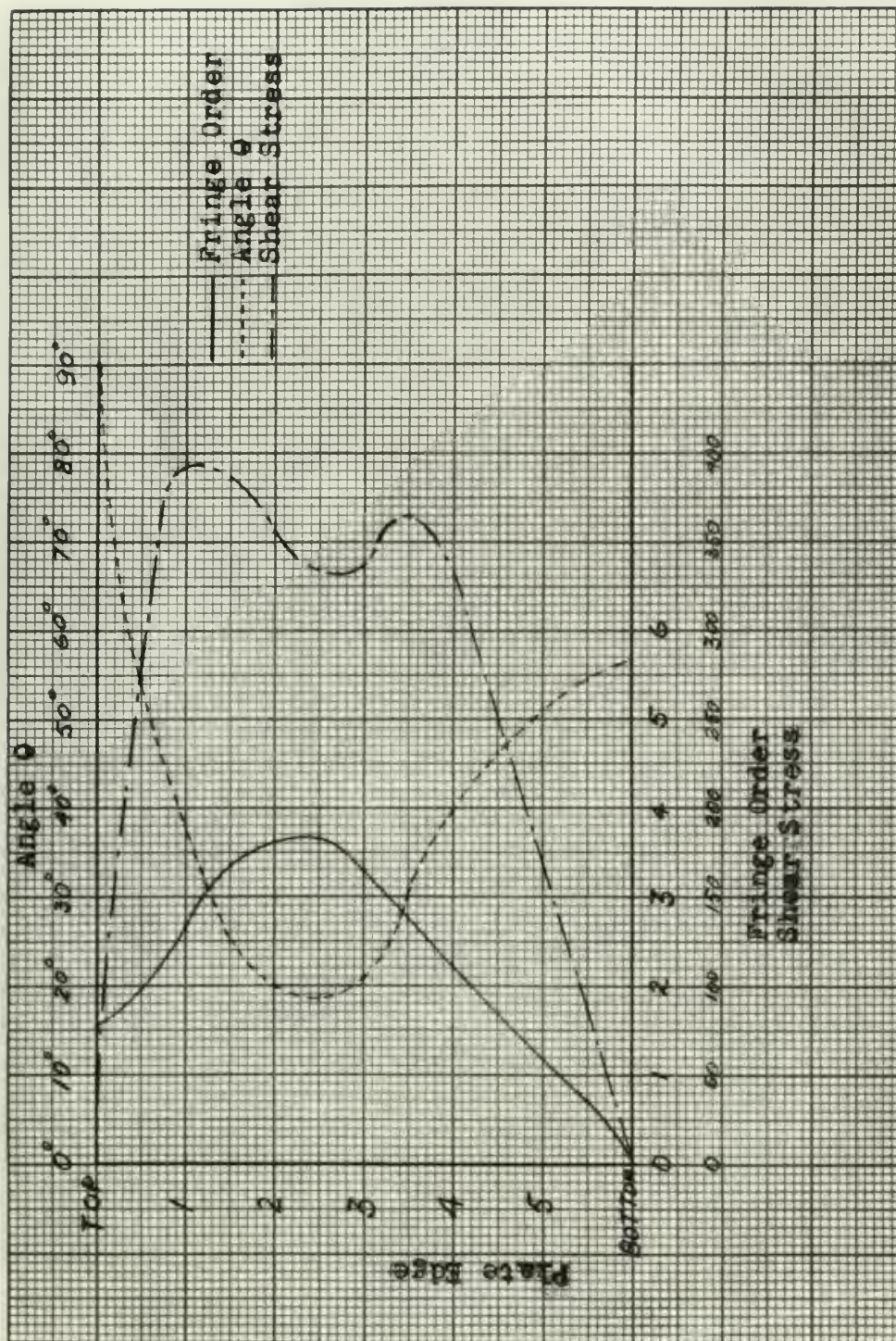


FIGURE IV
STIFFENED PLATE
Supported at sides and bottom
Load 1650 lbs

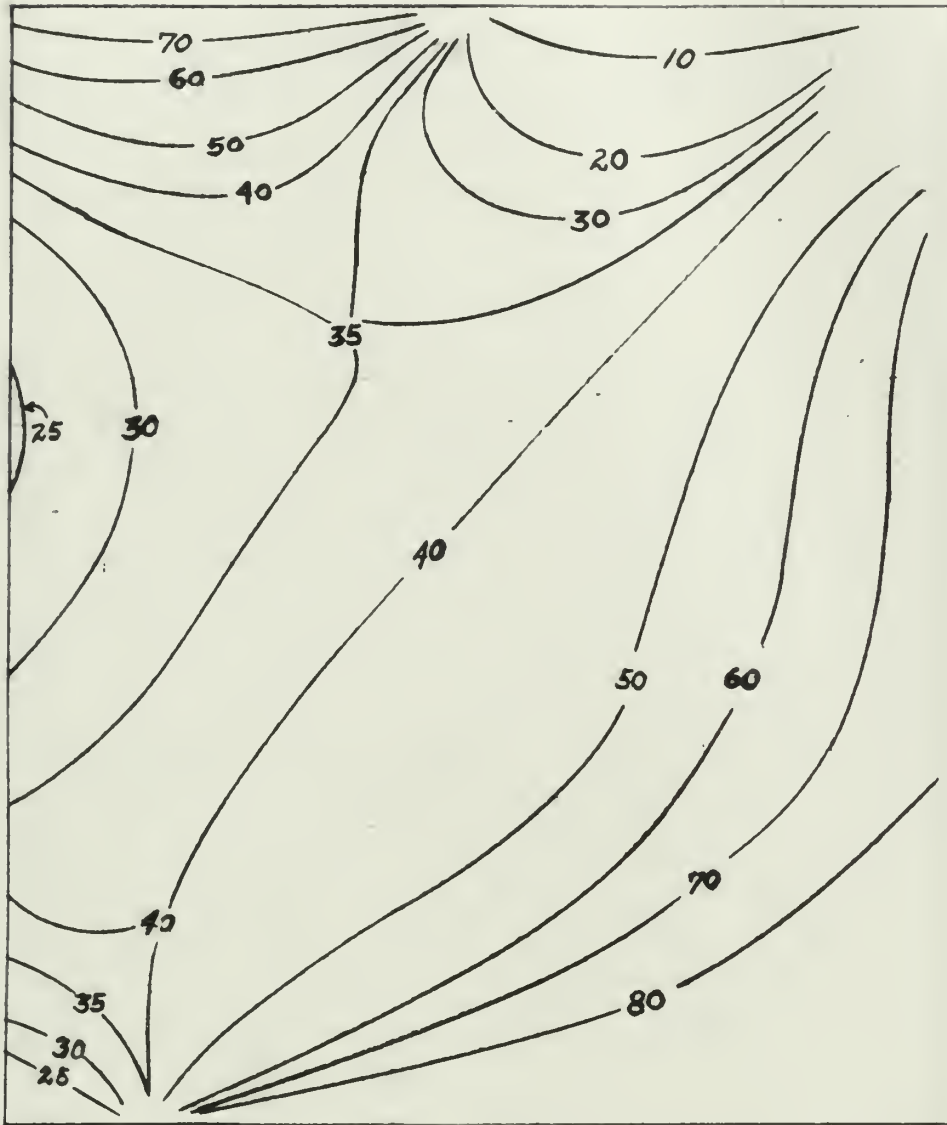


FIGURE V
ISOCLINIC PATTERN
Unstiffened Plate
Supported at sides only

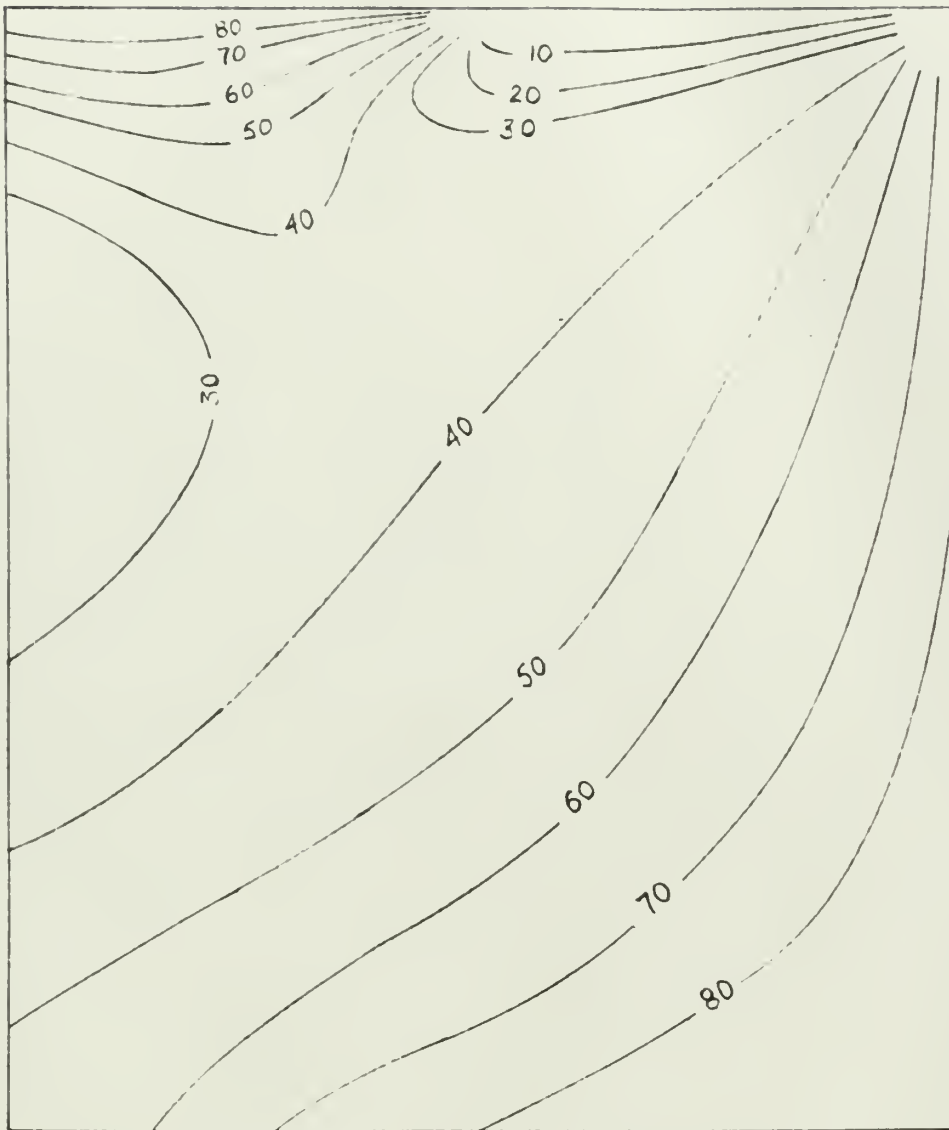


FIGURE VI
ISOCLINIC PATTERN
Unstiffened Plate
Supported at sides and bottom

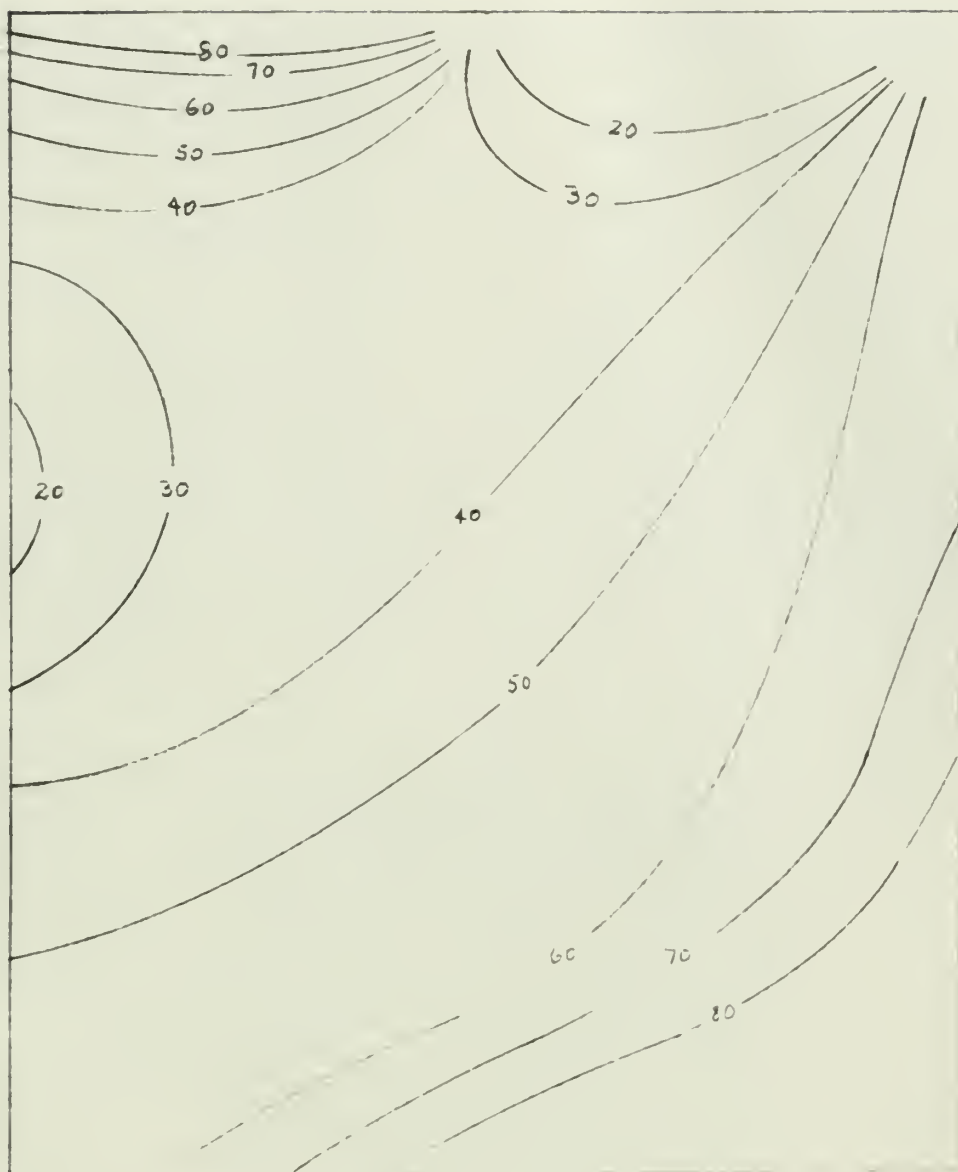


FIGURE VII
ISOCLINIC PATTERN
Stiffened Plate
Supported at sides and bottom

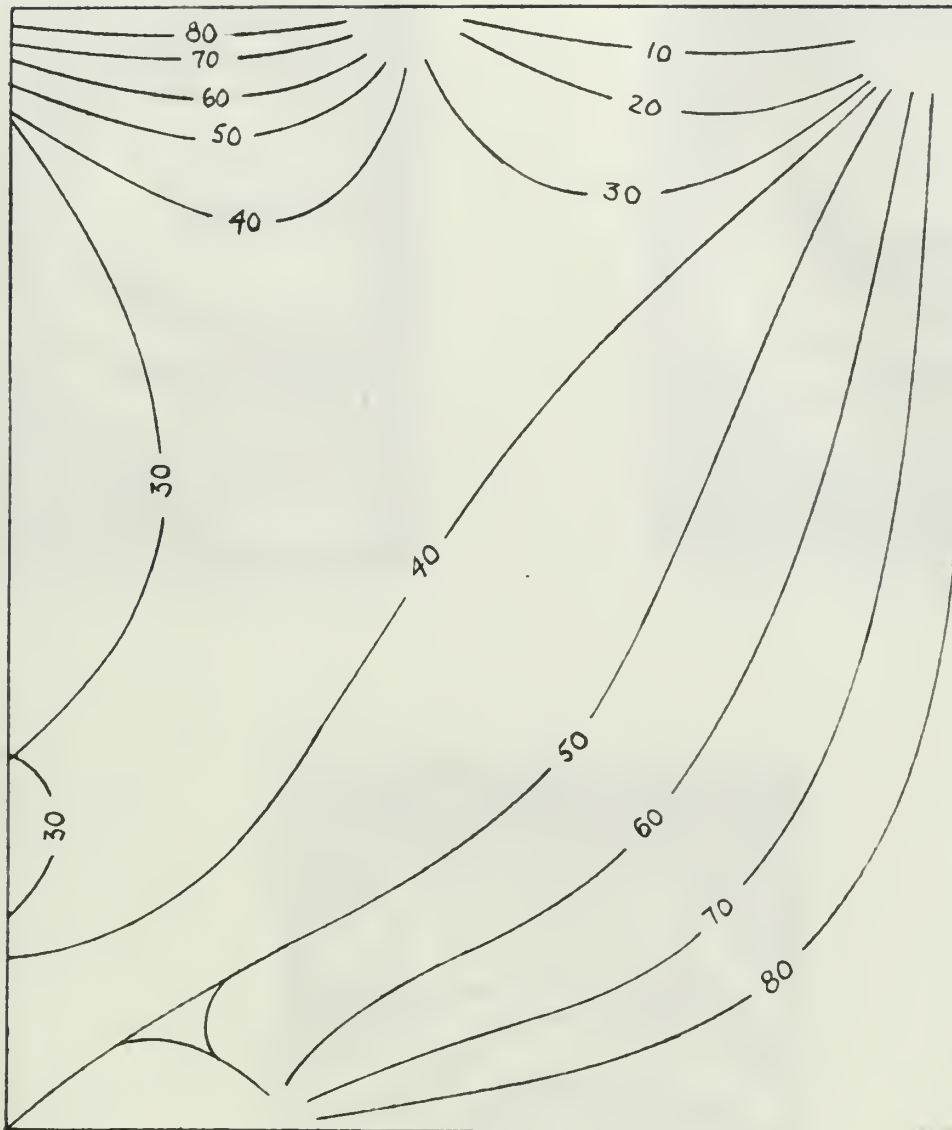


FIGURE VIII
ISOCLINIC PATTERN
Stiffened Plate
Supported at sides only



Edge - Light Field



Edge - Dark Field



Center - Dark Field

FIGURE IX
ISOCHROMATIC PATTERN
Unstiffened plate
Supported at sides only
Load 1650 lbs.



Edge - Light Field



Edge - Dark Field



Center - Dark Field

FIGURE X
ISOCHROMATIC PATTERN
Unstiffened plate
Supported at sides and bottom
Load 1650 lbs



Edge - Light Field



Edge - Dark Field



Center - Dark Field

FIGURE XI
ISOCROMATIC PATTERN
Stiffened Plate supported at sides and bottom
Load - 1050 lbs.

TABLE IV
LOAD PIN CALIBRATION

FOUR SR-4 TYPE A-7 WIRE STRAIN GAGES, G.F. - 1.91

BALDWIN STRAIN INDICATOR SETTING: G.F. - 2.03

<u>Load</u>	<u>Reading</u>	<u>Strain</u>
0	12 - 0527	0
28.5	12 - 0499	28
52.0	12 - 0476	51
62.3	12 - 0464	63
101.0	12 - 0428	99
136.0	12 - 0391	135
173.5	12 - 0355	172
210.5	12 - 0320	207
247.5	12 - 0280	247
267.0	12 - 0261	266
286.1	12 - 0241	286
325.0	12 - 0205	322
368.5	12 - 0160	367
382.5	12 - 0146	381
408.5	12 - 0120	407

Calibration constant - 1.00 μ in/in per pound

TABLE IV

LOAD PIN CALIBRATION

FOUR 22-4 TYPE A-V WIRE STRAIN GAGES, G.P. - 1.91
 WELDING STRAIN INDICATOR SETTING, G.P. - 5.03

Load	Strain	Strain
0	0	0
28.5	12 - 0227	28
52.0	12 - 0433	51
62.3	12 - 0476	63
101.0	12 - 0434	99
126.0	12 - 0433	135
173.5	12 - 0331	171
210.5	12 - 0359	207
247.5	12 - 0320	247
267.0	12 - 0280	266
288.1	12 - 0261	288
325.0	12 - 0247	325
358.5	12 - 0202	360
362.5	12 - 0160	381
408.5	12 - 0146	407

Calibration constant - 1.02 x 10⁶ lbs per pound

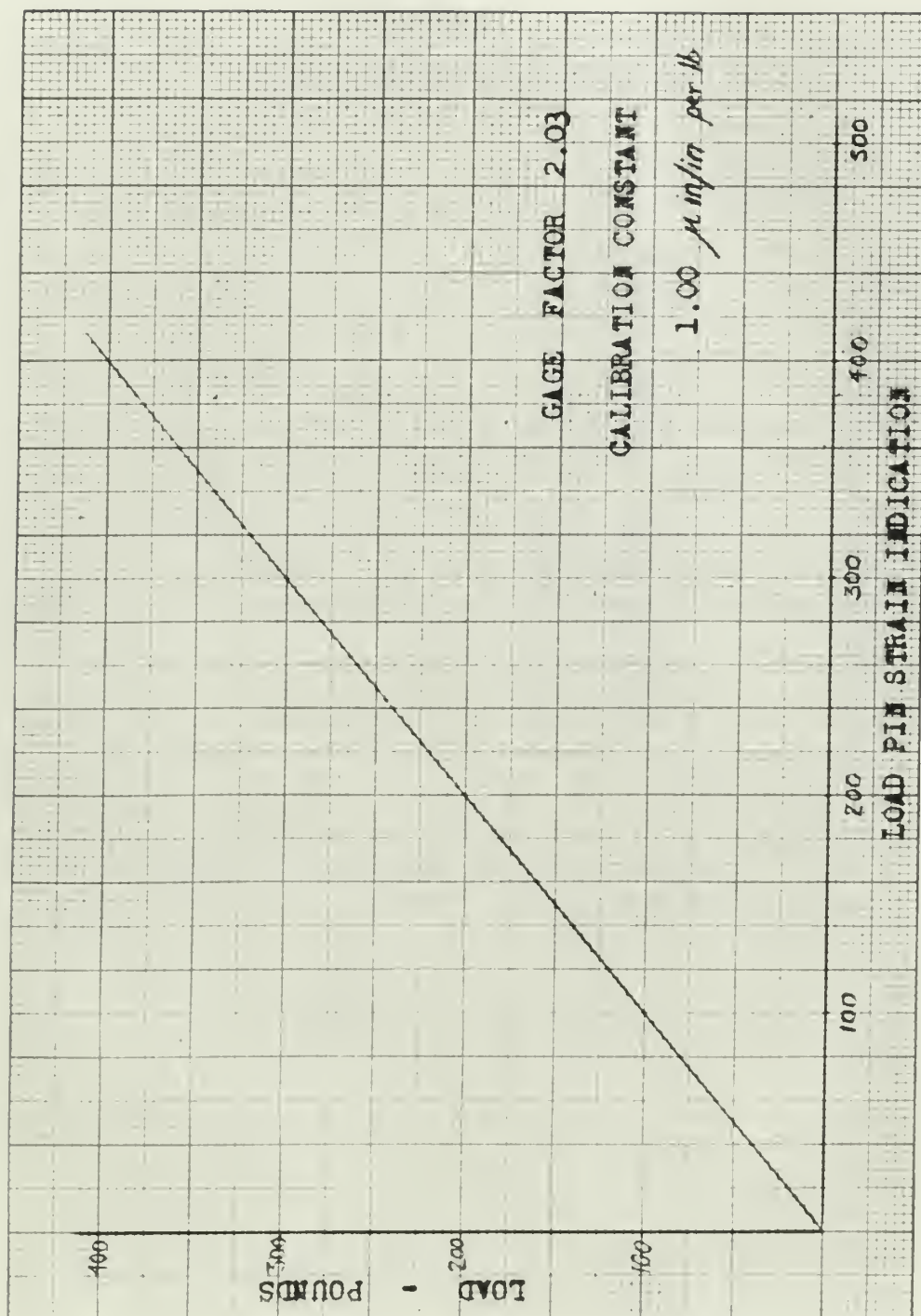


FIGURE XII
LOAD PIN CALIBRATION

TABLE V
FRINGE CONSTANT CALIBRATION

<u>Order</u>	<u>UP</u>	<u>Reading</u>	<u>Down</u>
0	10 - 0830		10 - 0825
1	10 - 1130		10 - 1125
2	10 - 1435		10 - 1425
3	10 - 1745		10 - 1750
4	12 - 0047		12 - 0058
5	12 - 0370		12 - 0370
6	12 - 0700		12 - 0700
0	10 - 0815		10 - 0810
1	10 - 1100		10 - 1100
2	10 - 1415		10 - 1410
3	10 - 1710		10 - 1715
4	12 - 0020		12 - 0035
5	12 - 0350		----
6	12 - 0655		12 - 0655

Calibration Constant - 310 μ -in/in/order

TABLE V

RELATION CONSTANT CALIBRATION

Order	UP	Reading	Down
0	12 - 0700	12 - 0700	12 - 0700
1	12 - 0720	12 - 0720	12 - 0720
2	12 - 0740	12 - 0740	12 - 0740
3	12 - 0760	12 - 0760	12 - 0760
4	12 - 0780	12 - 0780	12 - 0780
5	12 - 0800	12 - 0800	12 - 0800
6	12 - 0820	12 - 0820	12 - 0820
7	12 - 0840	12 - 0840	12 - 0840
8	12 - 0860	12 - 0860	12 - 0860
9	12 - 0880	12 - 0880	12 - 0880
10	12 - 0900	12 - 0900	12 - 0900
11	12 - 0920	12 - 0920	12 - 0920
12	12 - 0940	12 - 0940	12 - 0940
13	12 - 0960	12 - 0960	12 - 0960
14	12 - 0980	12 - 0980	12 - 0980
15	12 - 1000	12 - 1000	12 - 1000
16	12 - 1020	12 - 1020	12 - 1020
17	12 - 1040	12 - 1040	12 - 1040
18	12 - 1060	12 - 1060	12 - 1060
19	12 - 1080	12 - 1080	12 - 1080
20	12 - 1100	12 - 1100	12 - 1100
21	12 - 1120	12 - 1120	12 - 1120
22	12 - 1140	12 - 1140	12 - 1140
23	12 - 1160	12 - 1160	12 - 1160
24	12 - 1180	12 - 1180	12 - 1180
25	12 - 1200	12 - 1200	12 - 1200
26	12 - 1220	12 - 1220	12 - 1220
27	12 - 1240	12 - 1240	12 - 1240
28	12 - 1260	12 - 1260	12 - 1260
29	12 - 1280	12 - 1280	12 - 1280
30	12 - 1300	12 - 1300	12 - 1300

Calibration Constant - 310 u-in/in/ster

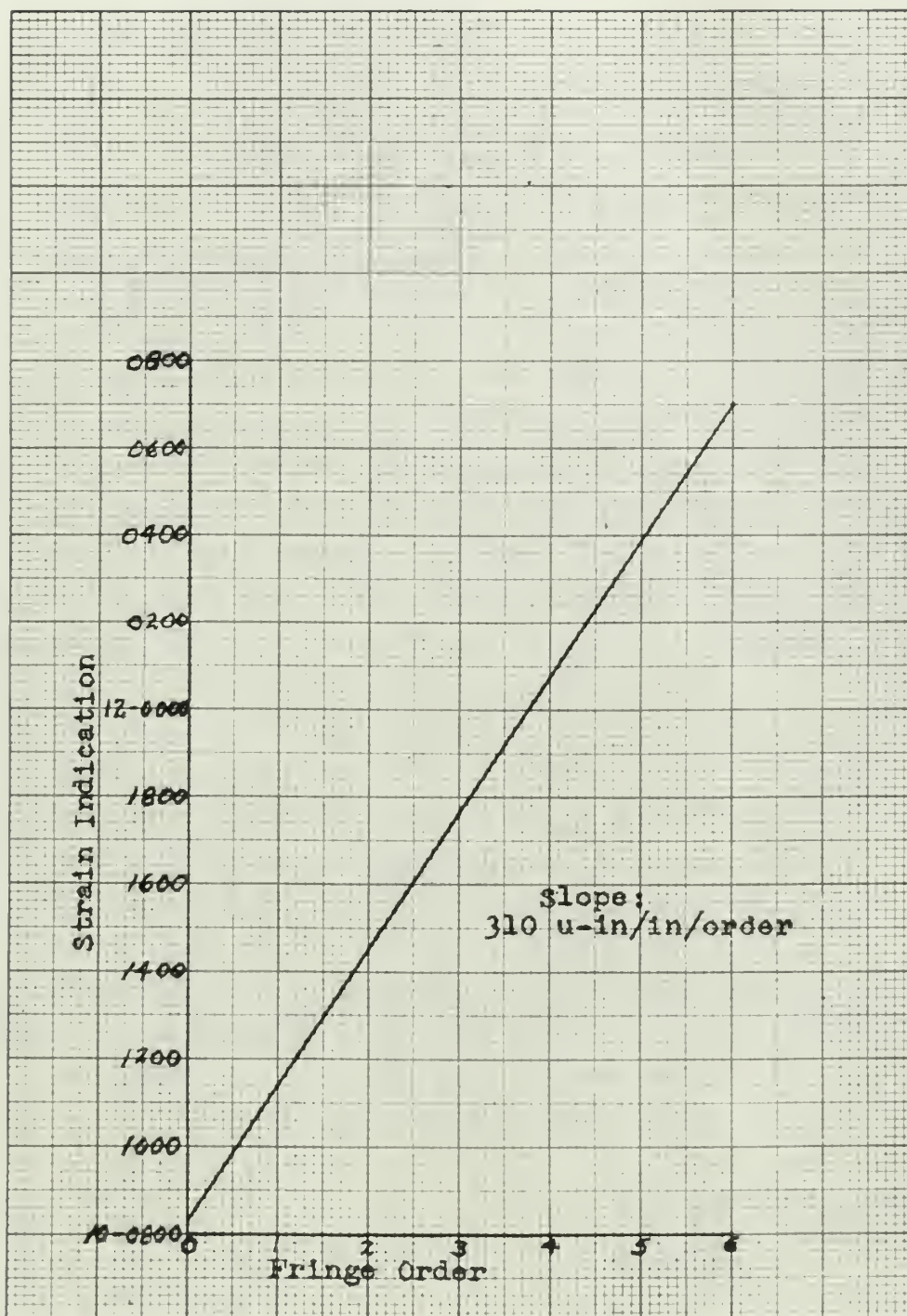


FIGURE XIII
FRINGE CONSTANT CALIBRATION

Figure (A)

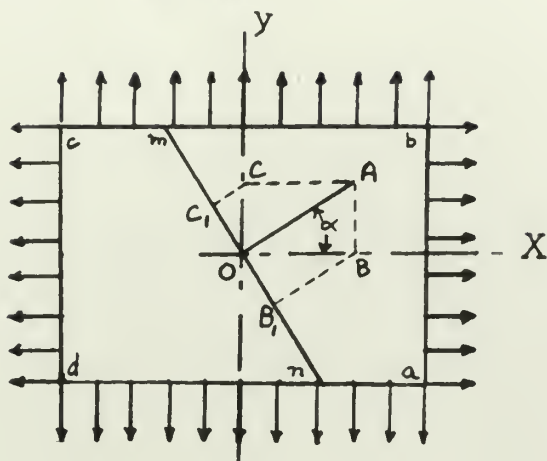


Figure (B)

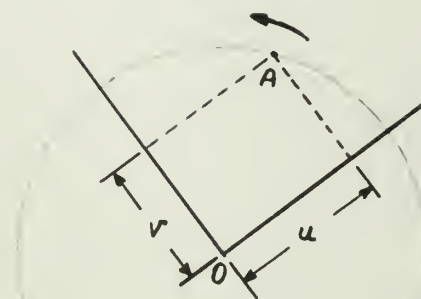
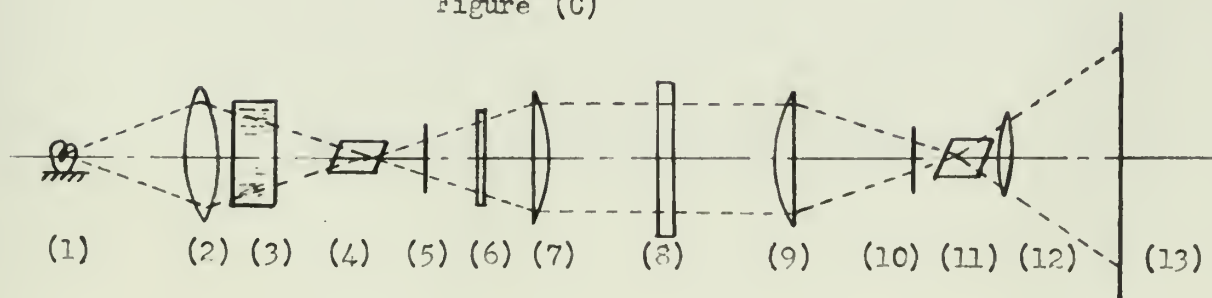


Figure (C)



- (1) Light Source
- (2) Condensing Lens
- (3) Cooler - Jar of Water
- (4) Nicol Prism Polarizer
- (5) Quarter-wave Plate
- (6) Color Filter
- (7) Lens
- (8) Stressed Model
- (9) Lens

- (10) Quarter-wave Plate
- (11) Nicol Prism Analyser
- (12) Lens
- (13) Screen or Camera Film

FIGURE XIV

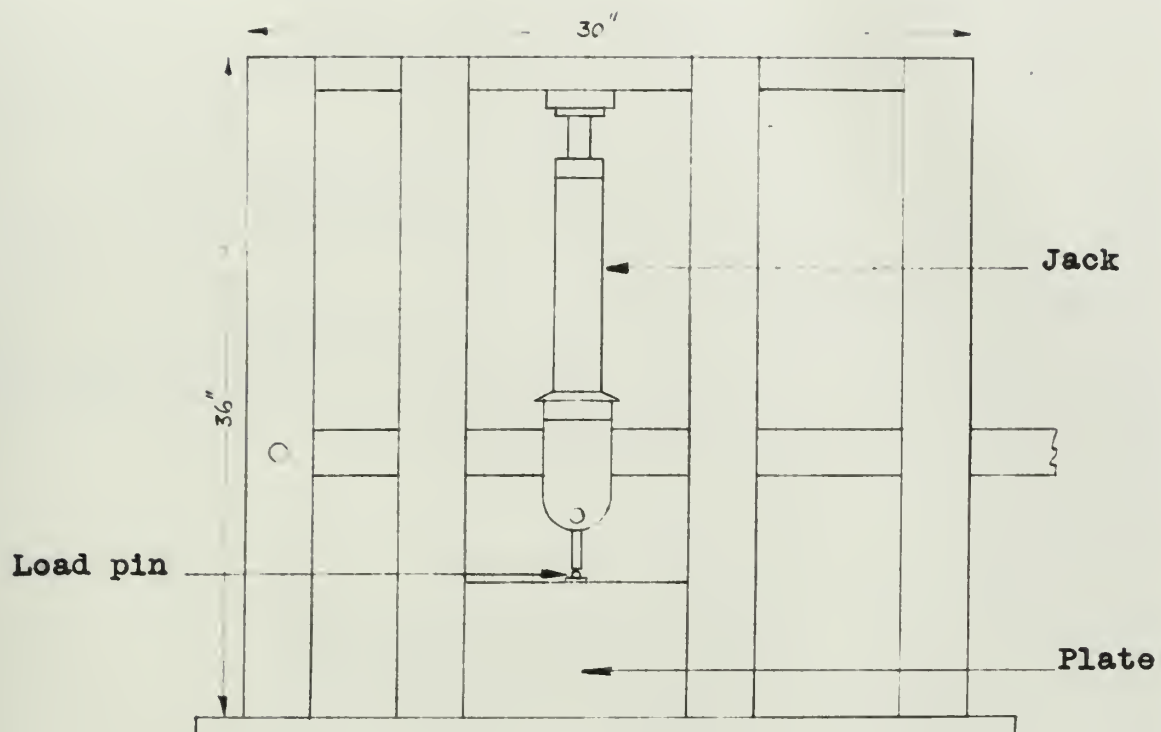


FIGURE XV
SCHEMATIC DRAWING OF LOAD FRAME

PHOTOGRAPHIC ILLUSTRATIONS

FIGURE XVI

General View of Polariscopes and
Load Frame

FIGURE XVII

Close-up of Load Frame

FIGURE XVIII

Tensile Model in Macklow-Smith
Loading Machine

FIGURE XIX

Close-up of Stiffened Catalin Plate
Model After Failure
(Note cracks resulting from restraint
caused by stiffener)

EXPERIMENTAL INVESTIGATION

FIGURE XVI

General View of Polariscope and
Lead Frame

FIGURE XVII

Close-up of Lead Frame

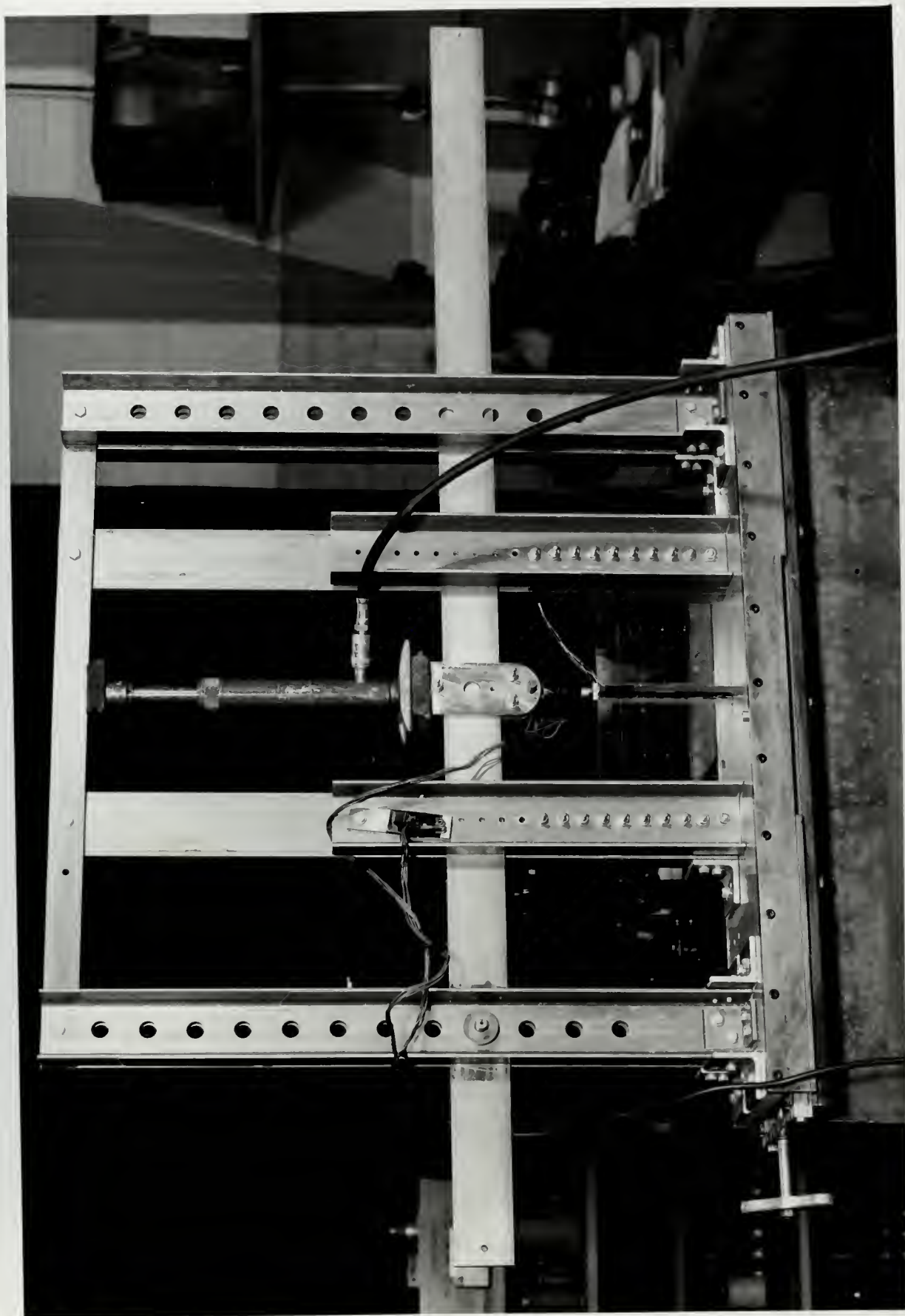
FIGURE XVIII

General View of Machine-Unit
Including Machine

FIGURE XIX

Close-up of Stiffened Detail Frame
Machine After Failure
(Note normal twisting from vibration
caused by failure)





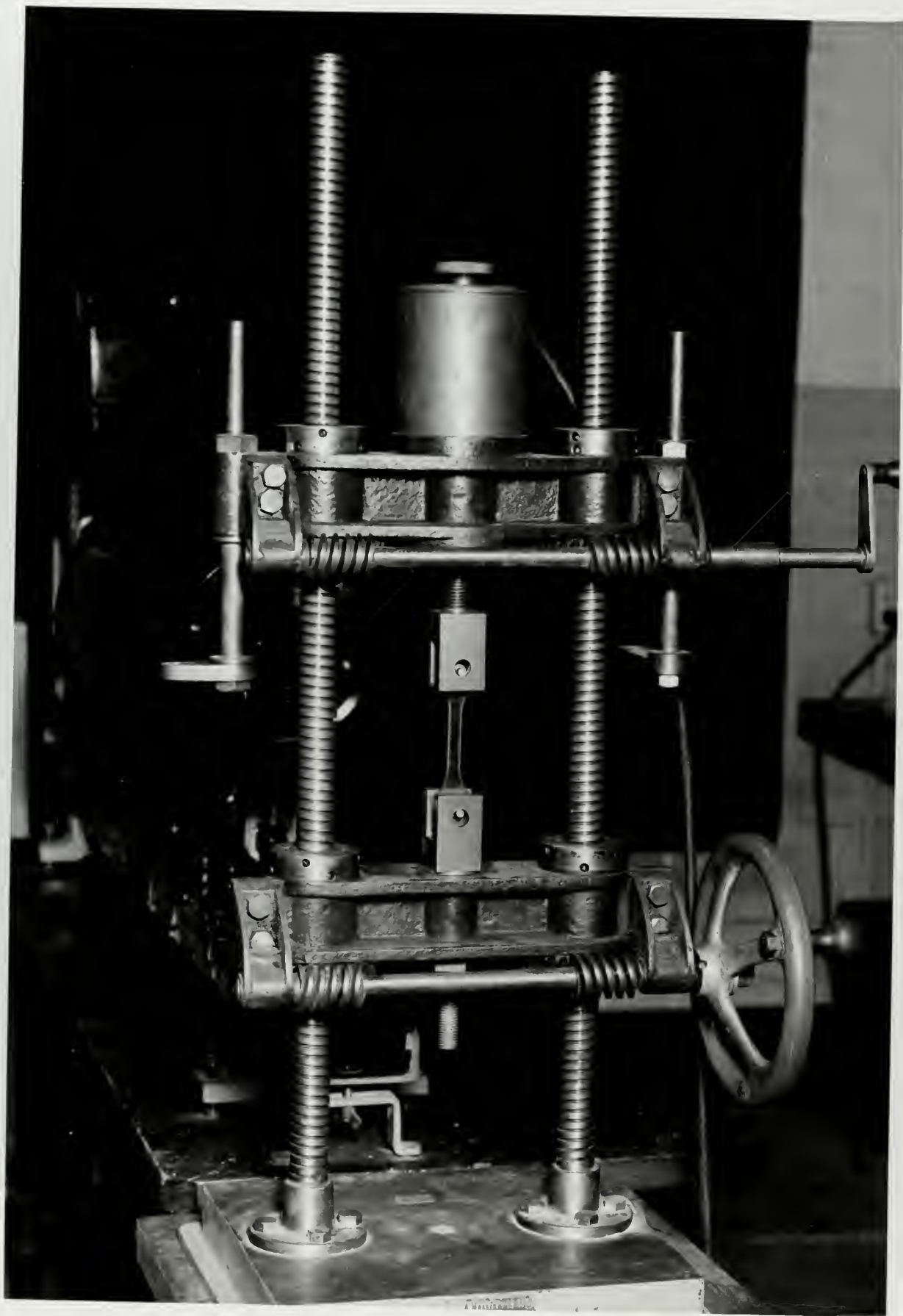




TABLE VI
STRAIN ON STIFFENER

<u>Load</u>		<u>Strain On Stiffener</u>	
<u>Reading</u>	<u>Actual Value</u> (lbs)	<u>Reading</u>	<u>Actual Value</u> (μ in/in)
12-0520	0	2-1025	0
12-0477	45	2-1095	70
12-0410	112	2-1210	185
12-0300	222	2-1370	345
12-0180	342	2-1500	475
12-0120	402	2-1660	635
12-0042	480	2-1730	705
10-1995	527	2-1890	865
10-1870	652	4-0000	975
10-1825	697	4-0030	1005
10-1690	832	4-0295	1270
10-1630	892	4-0370	1345
10-1555	967	4-0500	1475
10-1420	1102	4-0720	1695
10-1370	1152	4-0820	1795
10-1310	1212	4-0910	1885

Gage Factors:

Load Pin - 2.03

Stiffener - 1.91

TABLE VI STRAIN ON STIFFNESS

Reading	Load	Actual Value (lbs)	Reading	Strain On Stiffness Adjusted to 1 (in/in)
15-0350		0	5-1055	0
15-0477		45	5-1065	40
15-0470		115	5-1110	105
15-0300		225	5-1370	145
15-0180		345	5-1500	175
15-0120		400	5-1600	205
15-0045		480	5-1730	235
10-1035		555	5-1860	265
10-1030		625	4-0005	275
10-1055		685	4-0030	1005
10-1080		675	4-0055	1020
10-1030		805	4-0110	1045
10-1225		985	4-0200	1075
10-1430		1105	4-0250	1095
10-1570		1155	4-0300	1125
10-1310		1215	4-0310	1185

Scale Factor:
Load P/L = 2.0
Strain P/L = 1.0

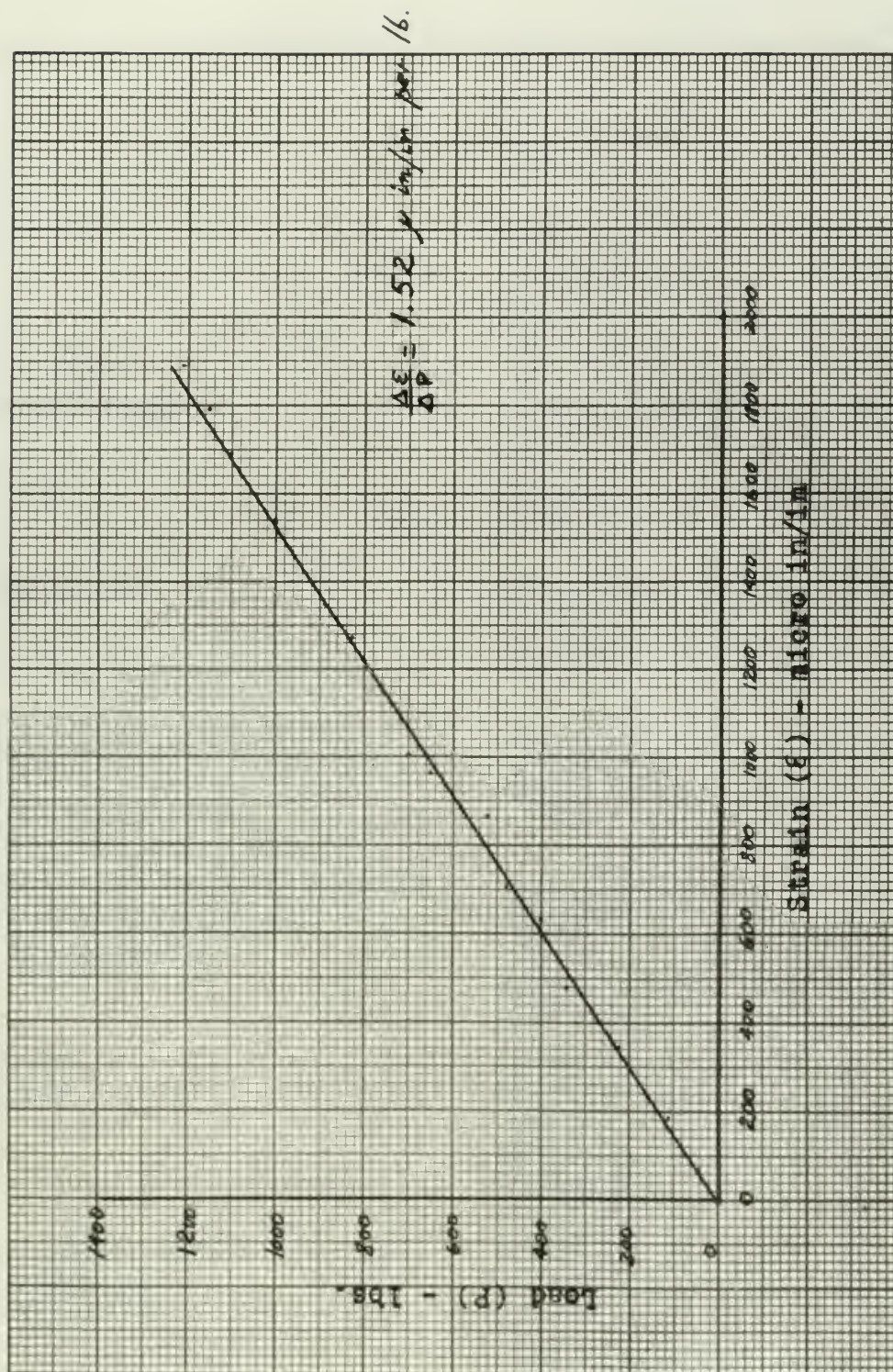


FIGURE XX
STRAIN ON STIFFENER

D. LITERATURE CITATIONS

- (1) Ballard, J.A. and Lennon, B.C. "An Investigation of the Effects of Shear on the Compressive Strength of Plating" - Thesis - Dept. Naval Arch. and Mar. Eng. - M.I.T., 1949.
- (2) Becker, H. "Photoelastic Analysis of a Spar Bulkhead in a Semi-Monocoque Airplane Fuselage" - Proc. of the Soc. Experimental Stress Analysis Vol. IV - No. I - 1946.
- (3) Bergman, S.G.A. "Behavior of Buckled Rectangular Plates under the Action of Shearing Forces" - Stockholm, Tekniska Hogskolan Avhandling, No. 56 - p. 166+ - 1948.
- (4) Brahtz, J.H.A. "Photoelastic Determination of Stresses" - Transaction of the Am. Soc. of Civil Engrs. - Vol. 102 1937.
- (5) Chow, L; Conway, H.D.; and Winter, G. "Stress in Deep Beams", Transactions of the American Society of Civil Engineers CXVIII; p. 686-702, 1953.
- (6) Conrad, R.D.; Hinners, R.A.; and Honsinger, L.V. "Stress Field of a Plane Plate Reinforced by a Longitudinal Girder and Subjected to Tension", Naval Architecture Department Thesis (Course XIII-A) - 1932.
- (7) Cox, H.L. "The Buckling of a Flat Rectangular Plate under Axial Compression and its Behavior After Buckling", Great Britain - Aeronautical Research Committee, Reports and Memoranda, No. 2041 - p. 26; London - H.M.S.O. - 1945.
- (8) Filon, L.N.G. "The Investigation of Stress in a Rectangular Bar by means of Polarized Light", Philosophical Magazine and Journal of Science, XXIII, p. 1-25; 1912.

BIBLIOGRAPHY

- (1) Willard, J.A. and Lemmon, H.C.
"An Investigation of the Effects of Stress on the Compressive Strength of Plastics" - Journal of Applied Polymer Science, Vol. 1, No. 1, p. 1-10, 1949.
- (2) Cooper, M.
"Photoelastic Analysis of a Stress Field in a Semi-Infinite Body" - Journal of Applied Polymer Science, Vol. 1, No. 1, p. 1-10, 1949.
- (3) Bergman, S.G.A.
"Behavior of Buckled Rectangular Plates under the Action of Shear" - Journal of Applied Polymer Science, Vol. 1, No. 1, p. 1-10, 1949.
- (4) Brainer, J.H.A.
"Photoelastic Determination of Stress" - Journal of Applied Polymer Science, Vol. 1, No. 1, p. 1-10, 1949.
- (5) Chow, L. Conway, H.D., and Winter, G.
"Stress in Deep Beams" - Journal of Applied Polymer Science, Vol. 1, No. 1, p. 1-10, 1949.
- (6) Conrad, R.D.; Hinners, R.A.; and Winkler, L.V.
"Stress Field of a Plane Plate Loaded by a Horizontal Load" - Journal of Applied Polymer Science, Vol. 1, No. 1, p. 1-10, 1949.
- (7) Cox, H.L.
"The Problem of a Thin Plate under Local Compression and its Behavior after Buckling" - Journal of Applied Polymer Science, Vol. 1, No. 1, p. 1-10, 1949.
- (8) Wilson, L.H.G.
"The Investigation of Stress in a Rectangular Bar by Means of Photoelastic Light" - Journal of Applied Polymer Science, Vol. 1, No. 1, p. 1-10, 1949.

- (9) Frocht, M. M. Photo-elasticity, Vol. I, New York: John Wiley and Sons, 1941.
- (10) Frocht, M. M. Photo-elasticity, Vol. II, New York: John Wiley and Sons, 1948.
- (11) Hamlin, W. G. "Suitability of Various Plastics for Stress Analysis by Photo-elasticity" - Thesis - Dept. of Civil and Sanitary Eng., M.I.T., 1941.
- (12) Hetenyi, M. Handbook of Experimental Stress Analysis, New York: John Wiley and Sons, 1950.
- (13) Holman, R. "A Photoelastic Study of the Stress Distribution in Stiffened Plating" - Thesis - Dept. of Naval Arch. and Marine Eng. - M.I.T. - 1955.
- (14) Murray, W. M. "Class Notes on Experimental Stress Analysis" - Course 2-126 Massachusetts Institute of Technology - 1956.
- (15) Murray, W. M. and Stein, P.K. "Strain Gage Technique" - Lectures and Laboratory Exercises - Massachusetts Institute of Technology - 1955.
- (16) Phillips, M. M. "The Tests of Bonding Materials for Bakelite 61-893" Thesis - Mechanical Eng. Dept. MIT - 1948.
- (17) Solakian, A. G. "Photoelastic Models with Cemented Elements" - Photo-elastic Journal, Vol. VI, No. 1 1938.
- (18) Timoshenko, S. and Goodier, J. N. Theory of Elasticity - New York - Mac Graw Hill - 1951
- (19) Timoshenko, S. and Mac Cullough, G. H. Elements of Strength of Materials - D. Van Nostrand Co., Inc., - New York - 1952.

(9) Frost, M. M.

(10) Frost, M. M.

(11) Frost, M. M.

(12) Frost, M. M.

(13) Frost, M. M.

(14) Frost, M. M.

(15) Frost, M. M. and
Gibson, P. K.

(16) Frost, M. M.

(17) Frost, M. M.

(18) Frost, M. M. and
Gibson, P. K.

(19) Frost, M. M. and
Gibson, P. K.

...
...
...
...
...

...
...
...
...
...

...
...
...
...
...

...
...
...
...
...

...
...
...
...
...

...
...
...
...
...

...
...
...
...
...

...
...
...
...
...

...
...
...
...
...

...
...
...
...
...

...
...
...
...
...

(20) Yamamoto, M. and
Kondo, K.

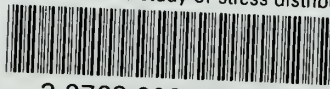
"Buckling and Failure of
Thin Rectangular Plates
in Compression" -- Tokyo
Imperial University -
Aero-resistance Institute
Report No. 119 - Vol. 10;
22 pp - 1935.

Page 11, Category (CS)
2, 0100

[illegible]

thesF425

A photo-elastic study of stress distribu



3 2768 002 00151 3

DUDLEY KNOX LIBRARY